1   **The Influence of Carbon Cycling on Oxygen Depletion in North-Temperate Lakes**
2

3   Austin Delany[1], Robert Ladwig[1], Cal Buelo[1], Ellen Albright[1], Paul C. Hanson[1]

4   [1] Center for Limnology, University of Wisconsin-Madison, Madison, WI, USA

5   *Correspondence to*: Austin Delany (addelany@wisc.edu)

6

7   **Abstract.** Hypolimnetic oxygen depletion during summer stratification in lakes can lead to

8   hypoxic and anoxic conditions. Hypolimnetic anoxia is a water quality issue with many

9   consequences, including reduced habitat for cold-water fish species, reduced quality of

10   drinking water, and increased nutrient and organic carbon (OC) release from sediments. Both

11   allochthonous and autochthonous OC loads contribute to oxygen depletion by providing

12   substrate for microbial respiration; however, their relative importance in depleting oxygen

13   across diverse lake systems remains uncertain. Lake characteristics, such as trophic state,

14   hydrology, and morphometry are also influential in carbon cycling processes and may impact

15   oxygen depletion dynamics. To investigate the effects of carbon cycling on hypolimnetic

16   oxygen depletion, we used a two-layer process-based lake model to simulate daily

17   metabolism dynamics for six Wisconsin lakes over twenty years (1995-2014). Physical

18   processes and internal metabolic processes were included in the model and were used to

19   predict dissolved oxygen (DO), particulate OC (POC), and dissolved OC (DOC). In our

20   study of oligotrophic, mesotrophic, and eutrophic lakes, we found autochthony to be far more

21   important than allochthony to hypolimnetic oxygen depletion. Autochthonous POC

22   respiration in the water column contributed the most towards hypolimnetic oxygen depletion

23   in the eutrophic study lakes. POC water column respiration and sediment respiration had

24   similar contributions in the mesotrophic and oligotrophic study lakes. Differences in source

1

25   of respiration are discussed with consideration of lake productivity and the processing and

26   fates of organic carbon loads.

27
28
29
30
31
32
33
34
35
36
37
38
39
40
41
42
43
44
45
46
47
48
49
50
51
52
53
54
55
56
57
58
59
60
61
62
63
64
65
66

2

1 Introduction

Hypolimnetic oxygen depletion is a persistent and global phenomenon that degrades lake ecosystems services (Nurnberg 1995; Cole & Weihe 2016; Jenny et al. 2016). In lakes where oxygen depletion results in hypoxia and even anoxia, habitat availability for cold-water fish species is eliminated (Magee et al. 2019), quality of drinking water is reduced (Bryant et al. 2011), and nutrient and OC release from lake sediments becomes elevated (Hoffman et al. 2013, McClure et al. 2020). An increase in the prevalence of hypolimnetic anoxia and associated water quality degradation in temperate lakes indicates the need to better understand how lake ecological processes interact with external forcings, such as hydrology and nutrient inputs, to control the development of anoxia (Jenny et al, 2016 a,b).

Allochthonous organic carbon (OC) loading to lakes that explains the prevalence of negative net ecosystem production (i.e., net heterotrophy) provides substrate for hypolimnetic oxygen depletion (Houser et al. 2003). Allochthonous OC sources have also been shown to influence dissolved oxygen (DO) and carbon dynamics in lakes by providing recalcitrant substrate for respiration (Cole et al. 2002; Hanson et al. 2014, Solomon et al. 2015). In lake surveys, dissolved allochthonous OC correlates positively with net heterotrophy ((Jansson et al. 2000), indicating the importance of allochthony to both the carbon balance and dynamics of dissolved gases (Prairie et al. 2002; Hanson et al. 2003). However, the persistent and often stable concentration of allochthonous DOC in the water column of lakes also indicates its recalcitrant nature, raising the question of whether allochthony alone can support high oxygen demand in the sediments and deeper waters of lakes.

3

91 The contributions of OC from autochthony to hypolimnetic oxygen depletion may be

92 important as well, despite its low concentrations relative to that of allochthonous OC in many

93 lakes (Cole et al. 2002). Autochthonous OC tends to be highly labile (Amon & Brenner 1996,

94 Thorpe & Delong 2002), and spot samples from lake surveys may not detect autochthonous

95 DOC, reducing its power as a correlate of ecosystem function. Positive correlation between

96 anoxia and lake phosphorus concentrations suggests autochthony may contribute

97 substantially to hypolimnetic oxygen demand (Rhodes et al. 2017; Rippey & McSorley,

98 2009; Jenny et al. 2016a,b); however, the link between nutrient concentrations, autochthony,

99 and hypolimnetic respiration is rarely quantified. Lakes with high autochthony can still be net

100 heterotrophic (Staehr et al. 2010; Cole et al. 2000), however, it matters where in the lake

101 autochthony is respired. Export of phytoplankton from the epilimnion to the hypolimnion and

102 sediments contributes to deep water oxygen demand (Müller et al. 2012; Rhodes et al. 2017;

103 Beutel 2003), and the magnitude and timing of organic carbon inputs to deeper waters in

104 lakes and the subsequent fate of that carbon deserves further exploration.

105
106 Understanding the relative importance of autochthony and allochthony to hypolimnetic

107 oxygen depletion requires consideration of a number of physical and biological processes

108 controlling oxygen sources and sinks in lakes (Hanson et al. 2015). For dimictic north

109 temperate lakes, the timing and dynamics of seasonal stratification determine the ambient

110 temperature and light conditions for metabolism and the extent to which the hypolimnion is

111 isolated from oxygen-rich surface waters (Snortheim et al. 2017, Ladwig et al. 2021). In

112 many lakes, the hypolimnion is below the euphotic zone, but in very clear lakes, primary

113 production within the hypolimnion may be an oxygen source (Houser et al. 2003). Lake

4

114   morphometry influences the spatial extents of stratified layers, which determines the ratio of

115   hypolimnetic volume to sediment surface area and the magnitude the sediment oxygen sink

116   for the hypolimnetic oxygen budget (Livingstone & Imboden 1996). Thus, the sources and

117   labilities of OC, lake morphometry, and lake hydrodynamics all contribute to hypolimnetic

118   oxygen budgets, making it an emergent ecosystem property with a plethora of causal

119   relationships to other ecologically important variables.

120
121   The availability of long-term observational data combined with process-based models

122   provides an opportunity to investigate OC sources and their control over the dynamics of lake

123   DO across multiple time scales. Long-term studies of lakes on regional and global scales

124   highlight how environmental trends can influence metabolic processes in lakes, and how

125   lakes can broaden our understanding of large-scale ecosystem processes (Richardson et al.

126   2017, Kraemer et al. 2017, Williamson et al. 2008). For example, long-term studies allow us

127   to investigate the impact that current and legacy conditions have on lake ecosystem function

128   in a given year (Carpenter et al. 2007). Process-based modeling has been used to investigate

129   metabolism dynamics and understand both lake carbon cycling (Hanson et al. 2004, Cardille

130   et al. 2007) and formation of anoxia (Ladwig et al. 2022); however, explicitly tying lake

131   carbon cycling and metabolism dynamics with long-term hypolimnetic DO depletion across a

132   variety of lakes remains largely unexplored. The combination of process-based modeling

133   with available long-term observational data, including exogenous driving data representative

134   of climate variability, can be especially powerful for recreating representations of long-term

135   lake metabolism dynamics (Staehr et al. 2010, Cardille et al. 2007).

136

5

137 In this study, our goal is to investigate OC source contributions to lake carbon cycling and

138 hypolimnetic oxygen depletion. We are particularly interested in the relative loads of

139 autochthonous and allochthonous OC to lakes and how they contribute to hypolimnetic DO

140 depletion across seasonal to decadal scales. We use a process-based lake metabolism model,

141 combined with daily external driving data and long-term limnological data, to study six lakes

142 within the North Temperate Lakes Long-Term Ecological Research network (NTL LTER)

143 over a twenty-year period (1995-2014). We address the following questions: (1) What are the

144 dominant sources of organic carbon that contribute to hypolimnetic oxygen depletion, and

145 how do their contributions differ across a group of diverse lakes over two decades? (2) How

146 does lake trophic state influence the processing and fates of organic carbon loads in ways that

147 affect hypolimnetic dissolved oxygen?

148

149 **2 Methods**

150 **2.1 Study Site**

151 This study includes six Wisconsin lakes from the NTL-LTER program (Magnuson et al.

152 2006). Trout Lake (TR), Big Muskellunge Lake (BM), Sparkling Lake (SP), and Allequash

153 Lake (AL) are in the Northern Highlands Lake District of Wisconsin and have been regularly

154 sampled since 1981 (Magnuson et al. 2006). Lake Mendota (ME) and Lake Monona (MO)

155 are in southern Wisconsin and have been regularly sampled by the NTL-LTER since 1995

156 (NTL-LTER, Magnuson et al. 2006). The NTL-LTER provides a detailed description of each

157 lake (Magnuson et al. 2006). The six lakes span gradients in size, morphometry, landscape

158 setting, and hydrology, which creates diverse carbon cycling characteristics and processes

159   across these systems. TR and AL are drainage lakes with high allochthonous carbon inputs

160   from surface water, while BM and SP are groundwater seepage systems with allochthony

161   dominated by aerial OC inputs from the surrounding landscape (Hanson et al. 2014). All four

162   northern lakes (TR, AL, BM, SP) are surrounded by a forested landscape. ME and MO are

163   both eutrophic drainage lakes surrounded by an urban and agricultural landscape. Although

164   the full range of DOC concentrations for lakes in northern Wisconsin varies from about 2 to

165   >30 mg L^{-1} (Hanson et al. 2007), DOC concentrations among our study lakes covered a

166   relatively narrow range typical of non-dystrophic lakes in Wisconsin (Hanson et al. 2007)

167   and are near the global averages previously estimated, i.e., 3.88 mg/L (Toming et al. 2020)

168   and 5.71 mg/L (Sobek et al. 2007), respectively. Morphometry, hydrology, and other

169   information can be found in Table 1.

170
171
172
173
174
175
176
177
178
179
180
181

7

182 **Table 1.** Physical and biogeochemical characteristics of the study lakes. The table includes
183 lake area (Area), maximum depth (Zmax), hydrologic residence time (RT), mean annual
184 temperature (Temp), mean annual surface total phosphorus concentration (Mean TP), and
185 mean annual surface DOC (Mean DOC).
186

Lake	Area (ha)	Zmax (m)	RT [3,4] (years)	Temp [2] (°C)	Mean TP [1] (µgL)	Mean DOC [1] (mgL)
Allequash Lake (AL)	168.4	8	0.73	10.5	14	3.9
Big Muskellunge (BM)	396.3	21.3	5.1	10.5	7	3.8
Sparkling Lake (SP)	64	20	8.88	10.6	5	3.12
Trout Lake (TR)	1607.9	35.7	5.28	9.8	5	2.8
Mendota (ME)	3961	25.3	4.3	12.5	50	5.6
Monona (MO)	1324	22.5	0.7	13.8	47	5.8

187
188 1 - Magnuson et al. (2020, 2006)
189 2 - Magnuson et al. (2022)
190 3 - Hunt et al. (2013)
191 4 - Webster et al. (1996)
192

193

194 **2.2 Driving Data and Limnological Data**

195 Most driving data for the model is provided by the "Process-based predictions of water

196 temperature in the Midwest US" USGS data product (Read et al. 2021). This includes lake

197 characteristic information such as lake area and hypsometry, daily modeled temperature

8

198   profiles, ice flags, meteorology data, and solar radiation for the six study lakes. Derived

199   hydrology data is used in calculating daily OC loading and outflow for the study lakes.

200   Hydrology for the northern lakes is taken from Hunt & Walker (2017), which was estimated

201   using a surface and groundwater hydrodynamic model. Hydrology for ME is taken from

202   Hanson et al. (2020), which used the Penn State Integrated Hydrologic Model (Qu & Duffy

203   2007). We assume for ME and MO that evaporation from the lake surface is approximately

204   equal to precipitation on the lake surface and that groundwater inputs and outputs to the lake

205   are a small part of the hydrologic budgets (Lathrop & Carpenter 2014). Therefore, ME

206   outflow is assumed to be equal to ME inflow. ME is the predominant hydrologic source for

207   MO (Lathrop & Carpenter 2014), thus, MO inflow is assumed to be equal to ME outflow,

208   and MO outflow is assumed to be equal to MO inflow. We found that the derived discharge

209   data for ME, TR, AL, and SP was approximately 20-50% higher than previously reported

210   values (Hunt et al. 2013, Webster et al. 1996), depending on the lake, while hydrology in BM

211   was approximately 25% too low (Hunt et al. 2013). To accommodate this issue, we adjusted

212   total annual hydrological inputs to match published water residence times for each lake

213   (Table 1), while retaining temporal hydrological patterns. NTL-LTER observational data are

214   interpolated to estimate daily nutrient concentration values, which are used in calculating

215   daily primary production in the model (Magnuson et al. 2020).

216

217   The NTL-LTER observational data used to calibrate and validate the model for the six lakes

218   include DO, DOC, and Secchi depth (Magnuson et al. 2020, Magnuson et al. 2022).

219   Saturation values for DO and gas exchange velocity used in calculating atmospheric
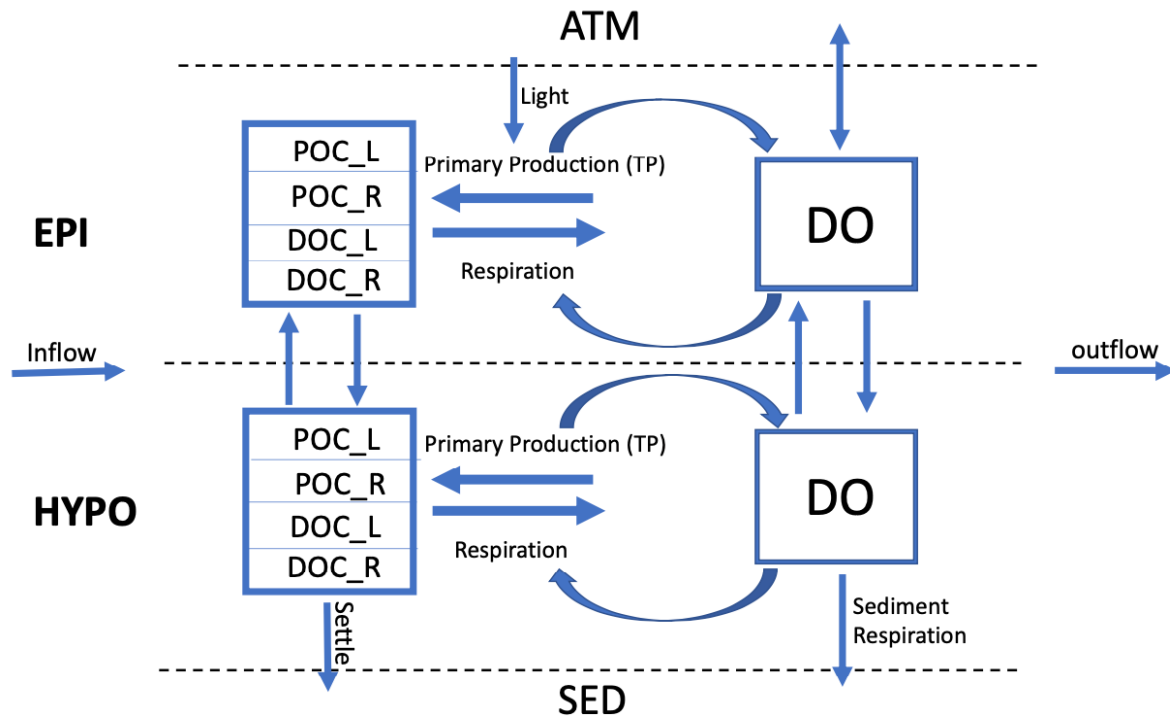
9

220 exchange for DO are calculated using the "o2.at.sat.base" and using the Cole and Caraco gas

221 exchange method from the "K600.2.KGAS.base" function within the USGS

222 "LakeMetabolizer" package in R (Winslow et al. 2016).

223

224 **2.3 The Model**

225 The goal of our model is to use important physical and metabolic processes involved in the

226 lake ecosystem carbon cycle to best predict DO, DOC, and POC, while keeping the model

227 design simple in comparison with more comprehensive water quality models (e.g., Hipsey et

228 al. 2022). We ran our model with a daily time step over a twenty-year period (1995-2014) for

229 each lake and included seasonal physical dynamics, such as lake mixing, stratification, and

230 ice cover from Read et al. 2021. Throughout each year, the model tracks state variables and

231 fluxes in the lake for each day (Fig. 1). These state variables include DO and the labile and

232 recalcitrant components of particulate organic carbon (POC) and dissolved organic carbon

233 (DOC). Initial conditions for each state variable are based on literature values or lake

234 observational data (SI Table 5). The model is initialized on January 1st of the first year, so

235 we set the initial labile POC mass to zero under the assumption that the concentration is low

236 in the middle of winter. The initial DO value is set to the saturation value based on the

237 conditions of the initial model run day and is calculated using the LakeMetabolizer R

238 package (Winslow et al. 2016). During stratified periods, the state variables and fluxes for

239 the epilimnion and hypolimnion are tracked independently. Atmosphere, sediments, and

240 hydrologic inputs and outputs are boundary conditions.

241

10

Figure 1. Conceptual lake model showing state variables (boxes) and fluxes (arrows). The model has two thermal layers under stratified conditions, as shown here, and tracks state variables separately for each layer. The sediment (SED), atmosphere (ATM), inflow and outflow are system boundaries. The state variables included are DO (dissolved oxygen), DOC_L (labile dissolved organic carbon), DOC_R (recalcitrant dissolved organic carbon), POC_L (labile particulate organic carbon), and POC_R (recalcitrant particulate organic carbon). Observed total phosphorus (TP) is used as a driving variable for primary production in the model.

The model is built specifically for this analysis; however, many of the assumptions around the model complexity and mathematical formulations are borrowed from literature cited (Ladwig et al. 2022, Hipsey et al. 2022, Hanson et al. 2014, McCullough et al. 2018). We chose to develop our own process-based model rather than use an existing model, such as GLM (Hipsey et al. 2022) or Simstrat (Goudsmit et al. 2002), so that we could simulate and measure the specific metabolism fluxes related to our study questions.

11

2.3.1 Stratification Dynamics

260

261 Lake physical dynamics are taken from the output of a previous hydrodynamic modeling

262 study on these same lakes over a similar time period (Read et al. 2021), which used the

263 General Lake Model (Hipsey et al. 2019). Before running the metabolism model, a

264 thermocline depth for each time step is estimated using derived temperature profiles for each

265 lake (Read et al. 2021) by determining the center of buoyancy depth (Read et al. 2011). After

266 calculating the thermocline depth, the volumes and average temperatures for each layer, and

267 the specific area at thermocline depth are determined using lake-specific hypsography. The

268 criteria for stratification include a vertical density gradient between the surface and bottom

269 layer of at least 0.05 kg m^{-3}, an average water column temperature above 4 °C, and the

270 presence of a derived thermocline (Ladwig et al. 2022). For any day that does not meet all of

271 these criteria, the water column is considered to be fully mixed. The thermocline depth

272 values are smoothed using a moving average with a window size of 14 days to prevent large

273 entrainment fluxes that can destabilize the model at very short time scales when thermal

274 strata are shallow. During mixed periods, the entire lake is treated as the epilimnion, and a

275 separate hypolimnion is not incorporated into the model dynamics. Ice cover in the model is

276 determined using the "ice flag" provided in the derived temperature profile data from Read et

277 al. (2021). Our metabolism model does simulate under-ice conditions, however we do not

278 include the presence of inverse stratification during winter periods.

279

2.3.2 External Lake and Environment Physical Fluxes

280

281 Atmospheric exchange of DO, external loading of OC, and outflow of OC are the three

282 environmental boundary fluxes accounted for in the water quality model (Table 3 Eq. 9-11).

283 The gas exchange velocity for atmospheric exchange is determined using the Cole and

284 Caraco model (1998) and is calculated using the LakeMetabolizer R package (Winslow et al.

285 2016). Oxygen saturation values are also calculated using this package. During ice covered

286 conditions, we assume that the atmospheric exchange value is ten percent of the value during

287 non-ice covered conditions based on sea ice gas exchange estimates (Loose and Schlosser,

288 2011).

289

290 For the northern lakes (TR, AL, BM, SP), we assume that allochthonous OC loads consist of

291 entirely recalcitrant substrates. We verify total OC load, total inflow concentration, and

292 recalcitrant OC export values with estimates from Hanson et al. (2014). For ME, we verify

293 the total annual allochthonous OC load and OC inflow concentrations against observed

294 inflow data from Hart et al. (2017) by back calculating inflow concentrations based on the

295 modeled OC equilibrium of the lake. MO inflow concentrations are equivalent to the in-lake

296 epilimnetic concentrations of OC from ME at each model time step. The total OC loads for

297 MO are verified based on the total allochthonous load found in McCullough et al. 2018.

298
299 **Table 2.** Equations for the model, organized by state variables, [*DO* (dissolved oxygen),
300 *DOCL* (labile dissolved organic carbon), *DOCR* (recalcitrant dissolved organic carbon),
301 *POCL* (labile particulate organic carbon), *POCR* (recalcitrant particulate organic carbon),
302 *Secchi*] and relevant fluxes. *Note:* The entrainment flux (*Entr*) is only included during
303 thermally stratified periods. The inflow (*IN*) and outflow (*OUT*) fluxes are not included in
304 the calculations for the hypolimnetic layer. The inflow of labile DOC (IN_{DOCL}) parameter in
305 Eq. 2 is only used for calculating allochthonous OC loads for MO. Atmospheric gas

13

306   exchange of dissolved oxygen (*AtmExch*) is not included for the hypolimnetic DO
307   calculation. Normalized total phosphorus is represented by (*TP_norm*). The volume (*V*) term
308   represents the respective lake layer volume, or the discharge volume for the inflow and
309   outflow equations. The term (*r_rate*) is included in Eq. 13 to represent the respiration rates of
310   the different OC pools. It is included to simplify the table of equations. Terms not defined
311   here are included in Table 3.
312

State Variables	
DO [gDO] $\frac{dDO}{dt} = (NPP * O2_{convert}) + AtmExch + Entr_{DO} - (R_{sed} * O2_{convert}) - (R_{wc} * O2_{convert})$	(1)
DOCL [gC] $\frac{dDOC_L}{dt} = (NPP * (1 - C_{NPP})) + IN_{DOCL} + Entr_{DOCL} - R_{DOCL} - OUT_{DOCL}$	(2)
DOCR [gC] $\frac{dDOC_R}{dt} = IN_{DOCR} + Entr_{DOCR} - OUT_{DOCR} - R_{DOCR\ Epi}$	(3)
POCL [gC] **Mixed and Epi:** $\frac{dPOC_L}{dt} = (NPP_{Epi} * C_{NPP}) + IN_{POCL} + Entr_{POCL} - R_{POCL\ Epi} - Settle_{POCL\ Epi} - OUT_{POCL}$ **Hypo:** $\frac{dPOC_L}{dt} = (NPP_{Hypo} * C_{NPP}) + Settle_{POCL\ Epi} - Settle_{POCL\ Hypo} - R_{POCL\ Hypo} - Ent_{POCL}$	(4) (5)
POCR [gC] **Mixed and Epi:** $\frac{dPOC_R}{dt} = IN_{POCR} + Entr_{POCR} - OUT_{POCR} - R_{POCR\ Epi} - Settle_{POCR\ Epi}$ **Hypo:** $\frac{dPOC_R}{dt} = Settle_{POCR\ Epi} - Settle_{POCR\ Hypo} - R_{POCR\ Hypo} - Entr_{POCR}$	(6) (7)
Secchi [m] $Secchi = \frac{1.7}{K_{LEC}}$	(8)
Fluxes	
Atm exchange [gDO d^{-1}] $AtmExch = K_{DO} * (DO_{sat} - DO_{prediction}) * Area_{sfc}$	(9)
Inflow [gC d^{-1}] $IN = Carbon\ Concentration_{inflow} * V_{inflow}$	(10)
Outflow [gC d^{-1}] $OUT = Carbon\ Concentration_{outflow} * V_{outflow}$	(11)
Net Primary Productivity [gC d^{-1}] $NPP = Pmax * (1 - e^{(-IP * \frac{Light}{Pmax})}) * TP_{norm} * \theta_{NPP}^{(T-20)} * V$	(12)
Respiration [gC d^{-1}] $R_{wc} = Carbon\ Pool * r_{rate} * \theta_{Resp}^{(T-20)} * \frac{DO_{Concentration}}{DO_{1/2} + DO_{Concentration}}$	(13)
Sediment Respiration [gC d^{-1}] $R_{sed} = r_{sed} * \theta_{Resp}^{(T-20)} * \frac{DO_{Concentration}}{DO_{1/2} + DO_{Concentration}} * Area_{sed}$	(14)
POC settle [gC d^{-1}] $Settle = (POC\ Pool * K_{POC}) * \frac{Area}{V}$	(15)

14

Entrainment [gC d^{-1}] $V_{Entr} = V_{epi}(t) - V_{epi}(t-1)$	(16)
$\quad V_{Entr} > 0$ (Epilimnion growing) $\qquad Entr = \frac{V_{Entr}}{V_{Hypo}} * Carbon\ Pool_{Hypo}$	(17)
$\quad V_{Entr} < 0$ (Epilimnion shrinking) $\qquad Entr = \frac{V_{Entr}}{V_{Epi}} * Carbon\ Pool_{Epi}$	(18)
Light [W m^{-2}] $Light = \int_{z_1}^{z_2}(I_{z_1} * e^{-(K_{LEC} * z)})\, dz * (1 - \alpha)$	(19)
Light Extinction Coefficient [Unitless] $K_{LEC} = LEC_{water} + (LEC_{POC} * ((\frac{POCL}{V}) + (\frac{POCR}{V}))) + (LEC_{DOC} * ((\frac{DOCL}{V}) + (\frac{DOCR}{V})))$	(20)

313

2.3.3 Internal Lake Physical Fluxes

315 The two in-lake physical fluxes included in the model are POC settling and entrainment of all

316 state variables. POC settling is the product of a sinking rate (m d^{-1}) and the respective POC

317 pool (g), divided by the layer depth (m) (Table 3 Eq. 15). Sinking rates are either borrowed

318 from literature values (Table 3) or fit during model calibration (see below). Entrainment is

319 calculated as a proportion of epilimnetic volume change (Table 2 Eq. 17-18). A decrease in

320 epilimnetic volume shifts mass of state variables from the epilimnion into the hypolimnion,

321 and an increase in volume shifts mass from the hypolimnion to the epilimnion.

322
323
324

15

325 **Table 3.** Model Parameters, grouped into three categories: constants, which are values that
326 were not tuned; manually calibrated, which are parameters manually tuned, typically guided
327 by ranges from the literature; and parameters calibrated through constrained parameter
328 search, which are calibrated through an automated search of parameter space.
329

Parameter	Abbreviation	Value	Units	Source
Constants				
Conversion of Carbon to Oxygen	$O2_{convert}$	2.67	Unitless	Mass Ratio of C:O
Respiration rate of DOCR	r_{DOCR}	0.001	day^{-1}	(Hanson et al., 2011)
Respiration rate of POCR	r_{POCR}	0.005	day^{-1}	Taken from ranges provided in (Hanson et al. 2004)
Respiration rate of POCR	r_{POCR}	0.005	day^{-1}	Taken from ranges provided in (Hanson et al. 2004)
Respiration rate of POCL	r_{POCL}	0.2	day^{-1}	Taken from ranges provided in (Hipsey et al. 2022)
Michaelis-Menten DO half saturation coefficient	$DO_{1/2}$	0.5	$g\ m^{-3}$	Taken from ranges provided in (Hipsey et al. 2022)
Light extinction coefficent of water	LEC_{water}	0.125	m^{-1}	Taken from ranges in Hart et al. (2017)
Ratio of DOC to POC production from NPP	C_{NPP}	0.8	Unitless	Biddanda & Benner (1997)
Albedo	α	0.3	Unitless	Global average (Marshall & Plumb, 2008)
Atmospheric gas exchange adjustment during ice covered conditions	C_{winter}	0.1	Unitless	Taken from ranges in (Loose & Schlosser, 2011)
Coefficient of light transmitted through ice	C_{ice}	0.05	Unitless	Taken from ranges provided in (Lei et al. 2011)
Settling velocity rate of POC_R	K_{POCR}	1.2	$m\ day^{-1}$	Taken from ranges found in (Reynolds et al.1987)

16

Parameter	Abbreviation	Value	Units	Source
Settling velocity rate of POC_L	K_{POCL}	1	$m \; day^{-1}$	Taken from ranges ranges found in (Reynolds et al.1987)
Temperature scaling coefficient for NPP	θ_{NPP}	1.12	Unitless	Taken from values provided in (Hipsey et al. 2022) and (Ladwig et al. 2022)
Temperature scaling coefficient for Respiration	θ_{Resp}	1.04	Unitless	Taken from values provided in (Hipsey et al. 2022) and (Ladwig et al. 2022)
Manually calibrated				
Light extinction of DOC	LEC_{DOC}	0.02 - 0.06	$m^2 g^{-1}$	Manually calibrated based on observed Secchi Depth ranges for the study lakes
Light extinction of POC	LEC_{POC}	0.7	$m^2 g^{-1}$	Manually calibrated based on observed Secchi Depth ranges for the study lakes
Maximum Daily Productivity	$Pmax$	0.5-5	$g \; m^{-3} day^{-1}$	Manually calibrated from mean productivity values from Wetzel (2001)
Recalcitrant DOC inflow concentration	$DOCR_{inflow}$	5-10	$g \; m^{-3}$	Based on ranges found in (Hanson et al. 2014, McCullough et al. 2018, Hart et al. 2017)
Recalcitrant POC inflow concentration	$POCR_{inflow}$	2-5	$g \; m^{-3}$	Based on ranges found in (Hanson et al. 2014, McCullough et al. 2018, Hart et al. 2017)
Calibrated through constrained parameter search				
Slope of the irradiance/productivity curve	IP	0.045, 0.015	$gCd^{-1}(Wm^{-2})^{-1}$	Based on ranges found in (Platt et al. 1980) and tuned separately for each lake region (South, North)

Parameter	Abbreviation	Value	Units	Source
Sediment respiration flux	r_{SED}	0.05 – 0.4	$g\ \ m^{-2}day^{-1}$	Based on ranges found in (Ladwig et al. 2021) and (Mi et al. 2020) and fit independently for each lake
Respiration rate of DOCL	r_{DOCL}	0.015 - 0.025	day^{-1}	Based on ranges found in (McCullough et al. 2018) and fit for each lake independently

330

331 **2.3.4 Internal Lake Metabolism Fluxes**

332 The metabolism fluxes in the model are net primary production (NPP) and respiration (R).

333 Respiration includes water column respiration for each OC state variable in the epilimnion

334 and hypolimnion and is calculated at each time step as the product of the OC state variable

335 and its associated first order decay rate (Table 2, Eq. 13). Sediment respiration for the

336 hypolimnion during stratified periods and the epilimnion (entire lake) during mixed periods

337 is a constant daily rate that is individually fit for each lake. Note that we did not include

338 anaerobic carbon metabolism in our modeling approach and discuss potential shortcomings

339 in the discussion section. We assume inorganic carbon is not a limiting carbon source. In the

340 model, we consider any DO concentration less than 1 g DO m^{-3} to be anoxic (Nürnberg

341 1995).

342

343 NPP is tracked in both the epilimnion and hypolimnion. NPP is a function of light, total

344 phosphorus concentration, temperature, a maximum productivity coefficient (*Pmax*), and a

345 slope parameter defining the irradiance and productivity curve (*IP*) (Table 2 Eq. 12). Total

346 phosphorus concentration in a layer taken is from observational data for each lake

347 interpolated to the daily time scale. Maximum daily primary production rates were taken

18

348   from Wetzel (2001). As these maximum production rates are not phosphorus-specific but

349   subsume lake-specific nutrient concentrations, we multiplied them with time-transient,

350   normalized TP concentrations. Normalizing was done by removing the mean of observed TP

351   and dividing by TP variance. This allows us to retain the time dynamics of the normalized

352   TP, which we use to represent seasonal TP dynamics for each lake. The Arrhenius equation

353   provides temperature control for NPP, and we determined through model fitting a θ of 1.12.

354   All OC derived from NPP is assumed to be labile and is split between particulate and

355   dissolved OC production, with eighty percent produced as POC and twenty percent produced

356   as DOC. This ratio was determined through model fitting and is similar to previously

357   reported values (Hipsey et al. 2022). Average light in a layer is calculated for each day and is

358   dependent on the depth of a layer and the light extinction coefficient (Table 2 Eq. 19). During

359   ice covered conditions, average light is assumed to be five percent of the average non-ice

360   covered value (Lei et al. 2011).

361

362   Epilimnetic and hypolimnetic water column respiration is tracked independently for each OC

363   pool in the model. During mixed periods, there are four OC pools – DOCR, DOCL, POCR,

364   POCL. During stratified periods, those pools are split into a total of eight pools that are

365   tracked independently for the epilimnion and hypolimnion. Respiration is calculated as a

366   product of the mass of a respective variable, a first order decay rate coefficient, temperature,

367   and oxygen availability (Table 2 Eq. 13). The respiration decay rate coefficients are based on

368   literature values (Table 3) or were fit during model calibration. An Arrhenius equation is

369   used for temperature control of respiration, with θ_{Resp} equal to 1.04, which was determined

19

370   through manual model fitting. The respiration fluxes are also scaled by oxygen availability

371   using the Michaelis-Menten equation with a half saturation coefficient of 0.5 g DO m^{-3}, such

372   that at very low DO concentrations, the respiration flux approaches zero.

373

374   Sediment respiration is calculated from a constant daily respiration flux, adjusted for

375   temperature and oxygen availability, using the Arrhenius and Michaelis-Menten equations,

376   respectively (Table 2 Eq. 14). The mass of sediment OC is not tracked in the model. During

377   stratified periods, we assume that the majority of epilimnetic sediment area is in the photic

378   zone, and therefore has associated productivity from macrophytes and other biomass. It is

379   assumed that this background productivity and sediment respiration are of similar magnitude

380   and inseparable from water column metabolism, given the observational data. Therefore,

381   epilimnetic sediment respiration is not accounted for in the model during stratified

382   conditions. During mixed conditions, we assume that sediment respiration is active on all

383   lake sediment surfaces, which are assumed to be equivalent in area to the total surface lake

384   area. During stratified periods, we use the area at the thermocline as the sediment area for

385   calculating hypolimnetic sediment respiration.

386

387   **2.3.5 Other in-lake calculations and assumptions**

388   We calculate a total light extinction coefficient (LEC) for the epilimnion and hypolimnion.

389   The total LEC for each layer is calculated by multiplying the dissolved and particulate

390   specific LEC values with their respective OC state variable concentrations, combined with a

391   general LEC value for water (Table 2 Eq. 20). This total LEC value is used to calculate a

392   daily estimate of Secchi depth (Table 2 Eq. 8). The coefficients for the light extinction of

393   water, DOC, and POC are manually calibrated based on observed Secchi depth ranges for the

394   study lakes (Table 3, SI Table 5).

395

396   **2.4 Model Sensitivity and Parameter Calibration**

397   To better understand the sensitivities of the model output to parameter values, we performed

398   a sensitivity analysis of the model parameters using the global sensitivity method from

399   Morris (1991). The sensitivity analysis showed that there were nine parameters to which the

400   model was consistently sensitive across the six study lakes. This group included the ratio of

401   DOC to POC produced from NPP (C_{NPP}), the maximum daily productivity parameter

402   (*Pmax*), the inflow concentration of recalcitrant POC ($POCR_{inflow}$), the setting velocity of

403   recalcitrant POC (K_{POCR}), the temperature fitting coefficients for productivity and respiration

404   (θ_{NPP}, θ_{Resp}) the slope of the irradiance/productivity curve (*IP*), the sediment respiration flux

405   (r_{SED}), and the respiration rate of DOCL (r_{DOCL}). We chose a subset of the nine parameters to

406   include in the uncertainty analysis based on the following justifications. The model results

407   showed that recalcitrant substrates are of lesser importance for lake metabolism dynamics, so

408   we chose not to further investigate the uncertainty of the $POCR_{inflow}$ and K_{POCR} parameters.

409   The *Pmax* and *IP* parameters are directly correlated, so we chose to remove Pmax from

410   further uncertainty considerations. The θ_{NPP} and θ_{RESP} parameters act as substitutes for water

411   temperature, a well-known "master variable" in water quality modeling, and directly reflect

412   seasonality in the model. Therefore, we chose to omit these parameters for further

413   uncertainty calculations. The final subset of parameters for uncertainty analysis consisted of

21

414   C_{NPP}, r_{DOCL}, r_{SED}, and *IP*. Of the four parameters, we felt C_{NPP} was best constrained by the

415   literature. To reduce the number of parameters estimated in the calibration process we

416   restricted the automated constrained parameter search to the remaining three.

417
418   Model parameters are grouped into three categories: constants, manually calibrated, and

419   parameters calibrated through an automated constrained parameter search. The constant

420   parameters are consistent across the study lakes and are not tuned. The manually calibrated

421   parameters were allowed to vary by lake and are typically guided by ranges from the

422   literature. The constrained parameter search uses an automated search of parameter space,

423   constrained by literature values, to fit the *IP*, r_{SED}, and r_{DOCL} parameters for the study lakes.

424   Specifically, we performed a constrained fitting of the model to observational data using the

425   Levenberg-Marquardt algorithm within the "modFit" function of the "FME" R package

426   (Soetaert & Petzoldt, 2010).

427
428   The first 15 years of the model output was used for calibration and the last 5 years were used

429   for model validation. We chose the first 15 years for calibration because the observational

430   data were relatively stable and were not indicative of any large trends in ecosystem

431   processes, as opposed to the last five years which showed slightly more model deviation

432   from DOC observational data in the southern lakes (SI Fig. 2).

433

434   **2.5 Model Uncertainty**

435   Sensitivity guided the uncertainty analysis. To quantify uncertainty around model

436   predictions, we sampled *IP*, r_{SED}, and r_{DOCL} simultaneously from uniform distributions

22

437   defined by +-30% of the literature ranges used for our calibrated parameter values (Table 3).

438   We ran one hundred model iterations randomly sampling the three model state variables

439   across these distributions. We plotted the minimum and maximum values for these uniform

440   distributions and included them in the time series plots (Fig. 2, 3, 4, SI Fig. 1,2,3).
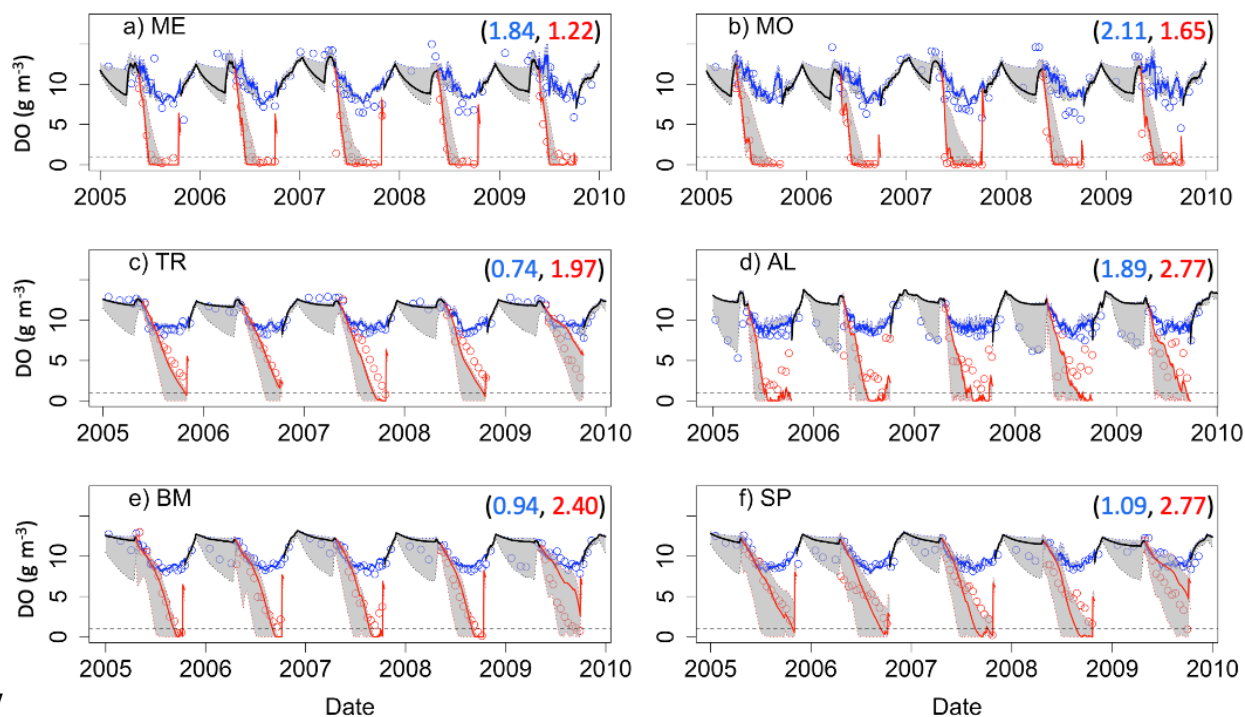
441
442

443   **3 Results**

444
445   **3.1 Model Fit to Ecosystem States**

446   Model predictions of DO reproduce observed seasonal variability well. Note that RMSE

447   values presented here represent model error combined over both the validation and

448   calibration periods (see Supplementary Material: Table S1 for calibration and validation

449   specific RMSE values), and that state variables are presented with truncated time ranges for

450   visual clarity (see Supplementary Material: Fig. S1-S3 for full time series). Epilimnetic DO

451   generally has lower RMSE than DO in the hypolimnion (Fig. 2). In the epilimnion, RMSE

452   ranges from 0.74 g DO m^{-3} (TR) to 2.11 g DO m^{-3} (MO), and in the hypolimnion, RMSE

453   ranges from 1.22 g DO m^{-3} (ME) to 2.77 g DO m^{-3} (AL, SP). Validation NSE values for DO

454   ranged from -1.45 (AL) to 0.02 (ME) in the epilimnion and -0.30 (SP) to 0.86 (ME) in the

455   hypolimnion. Validation KGE values for DO ranged from 0.40 (AL) to 0.90 (TR) in the

456   epilimnion and 0.35 (SP) to 0.80 (ME) in the hypolimnion. KGE and NSE values for all

457   lakes can be found in SI Table 7. In the southern lakes, modeled values reach anoxic levels

458   and generally follow the DO patterns recorded in the observed data (Fig. 2a-b).

459   Observational data for the northern lakes show an occasional late summer onset of anoxia,
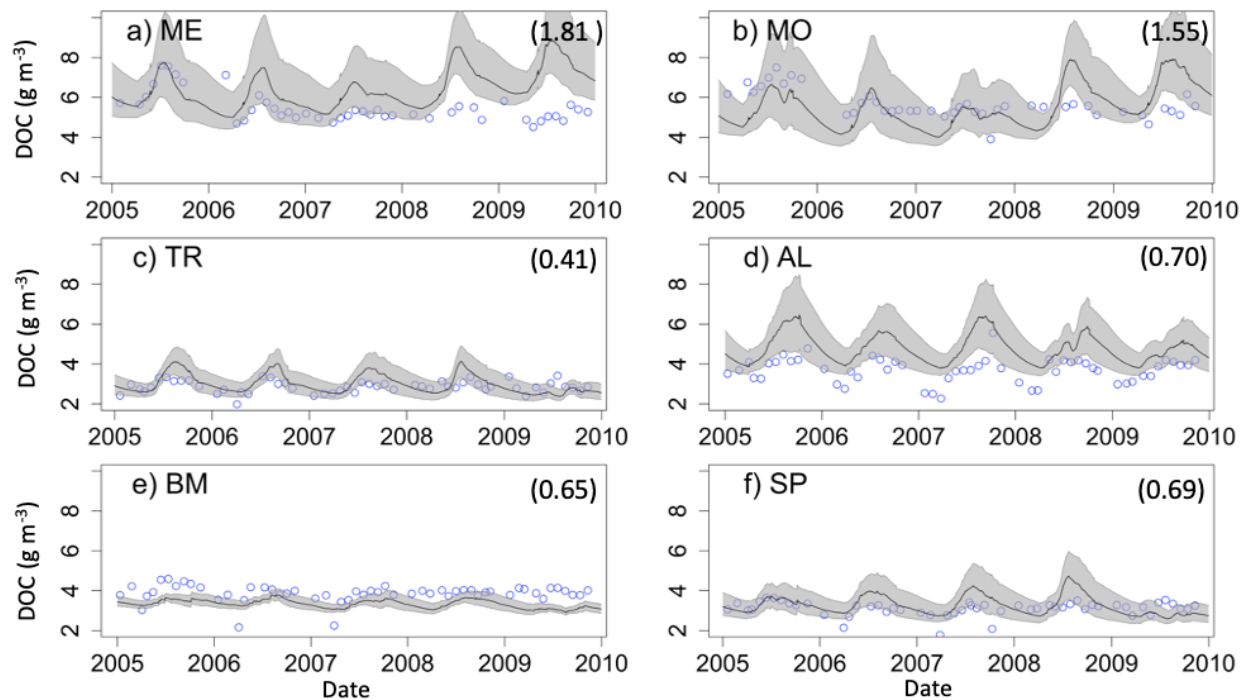
23

460 and these events are generally captured in the model output. A late summer spike in

461 hypolimnetic DO predictions commonly occurs as well, which is likely a model artifact

462 caused by the reduction of hypolimnetic volumes to very small values over short time periods

463 prior to fall mixing. Reduction to small volumes, coincident with modest fluxes due to high

464 concentration gradients, result in transient high concentrations. Overall, the goodness-of-fit

465 of hypolimnetic DO in our study lakes does not seem to follow any regional or lake

466 characteristic patterns.

467
468 **Figure 2.** Dissolved oxygen (DO) time series for the years, 2005-2010, for the six study
469 lakes (a-f). Model predictions are represented by lines, and circles represent the observational
470 data. Epilimnetic DO values are blue and Hypolimnetic DO values are red. Fully mixed
471 periods for the lake are indicated by a single black line. RMSE values (epilimnion,
472 hypolimnion; $g\ m^{-3}$) for the validation period are included in the upper right of each panel.
473 Uncertainty is represented by gray shading.
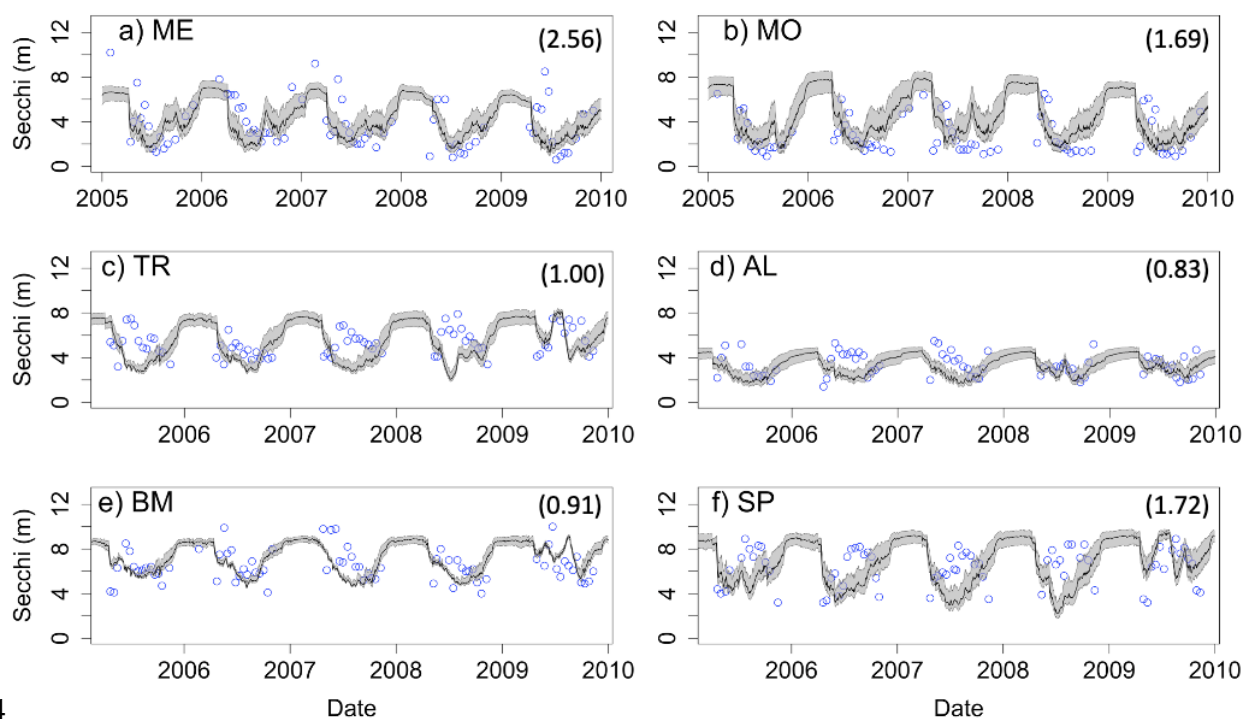
474

475

24

476   The two southern lakes (ME, MO) have epilimnetic DOC RMSE values greater than 1.00 g

477   C m^{-3}, while the RMSE for northern lakes ranges from 0.41 g C m^{-3} (TR) to 0.70 g C m^{-3}

478   (AL) (Fig. 3). In the southern lakes, NSE epilimnetic DOC values were below -3.00 and

479   KGE values ranged from -0.29 to -0.32. In the northern lakes, NSE values for DOC ranged

480   between -2.75 (SP) and -0.31 (AL). KGE values ranged from -0.07 (BM) to 0.35 (TR). All

481   NSE and KGE metrics for DOC can be found in SI Table 7. Observational data in both

482   southern lakes indicate a decrease in DOC concentration beginning around 2010, which is

483   largely missed in the model predictions (Fig.3a-b, Supplementary Material: Fig. S2a-b) and

484   cause an overestimation of DOC by about 1-2 g C m^{-3}. However, model predictions converge

485   with observed DOC toward the end of the study period (Supplementary Material: Fig. S2a-

486   b). In AL, the seasonal patterns of modeled DOC are smaller in amplitude than the

487   observational data (Supplementary Material: Fig. S2d).

488

Figure 3. Epilimnetic dissolved organic carbon (DOC) time series for the years, 2005-2010, for the six study lakes (a-f). Model predictions are represented by lines, and circles represent the observational data. RMSE values for the validation period are included for each lake (g C m^{-3}). Uncertainty is represented by gray shading.

Secchi depth predictions reproduce the mean and seasonal patterns in all lakes (Fig. 4). Although the model produced annual cycles of Secchi depth that generally covered the range of observed values, short term deviations from annual patterns in the observed data are not reproduced. The timing of minima and maxima Secchi depth sometimes differed between predicted and observed values for the northern lakes. In addition, winter extremes in observed Secchi depth are not always reproduced by the model, which is especially evident for ME (Fig. 4a). However, winter observational data for Secchi are more sparse than other seasons.
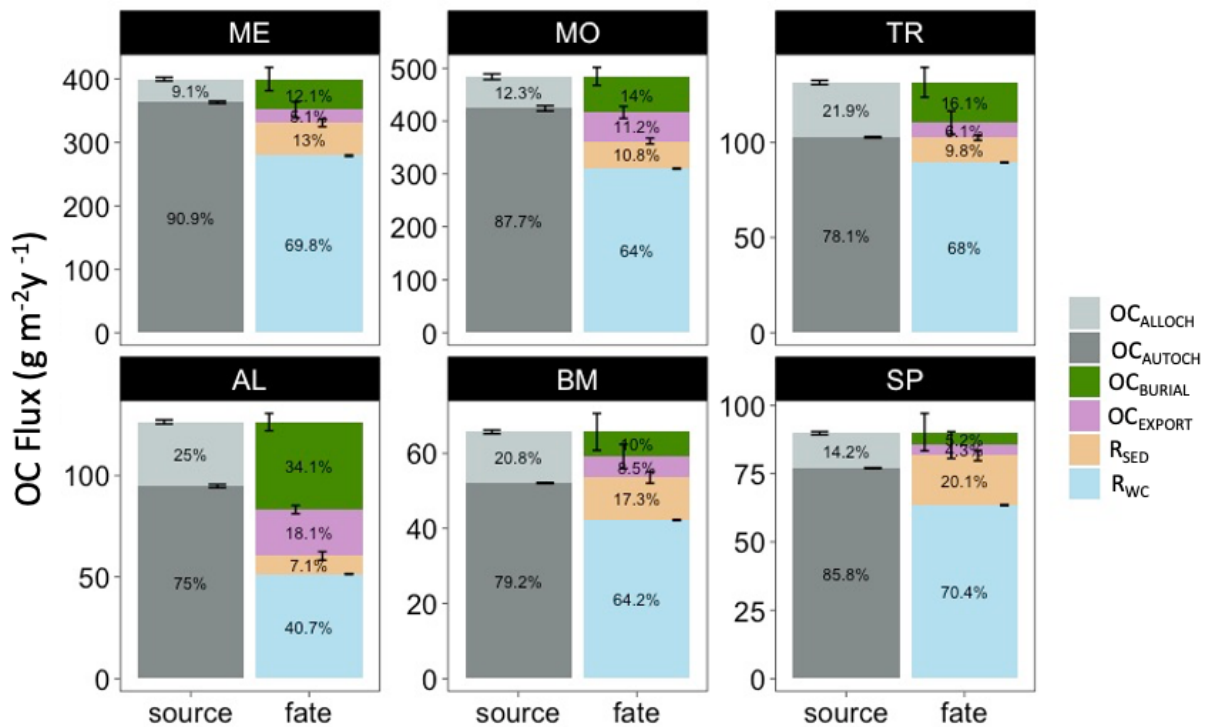
26

504
505 **Figure 4.** Secchi depth time series for the years, 2005-2010, for the six study lakes (a-f).
506 Model predictions are represented by lines, and circles represent the observational data.
507 RMSE values for the validation period are included for each lake (m). Uncertainty is
508 represented by gray shading.
509

510 **3.2 Ecosystem Processes**

511 The mean annual OC budgets of all six lakes show large differences in the sources and fates

512 of OC among lakes (Fig. 5; Supplementary Material: Table S3). Autochthony is the dominant

513 source of OC for all study lakes. Water column respiration is the largest portion of whole-

514 lake respiration in ME, MO, TR, SP, and BM. Sediment respiration contributions are a lower

515 proportion of total respiration in ME, MO, and TR (mean of 14.1%), and are slightly higher

516 in BM and SP (mean of 18.7%). AL has a more even distribution of OC fates. OC burial

517 amounts also vary across the study lakes, with the highest percentage in AL (34.1%), and
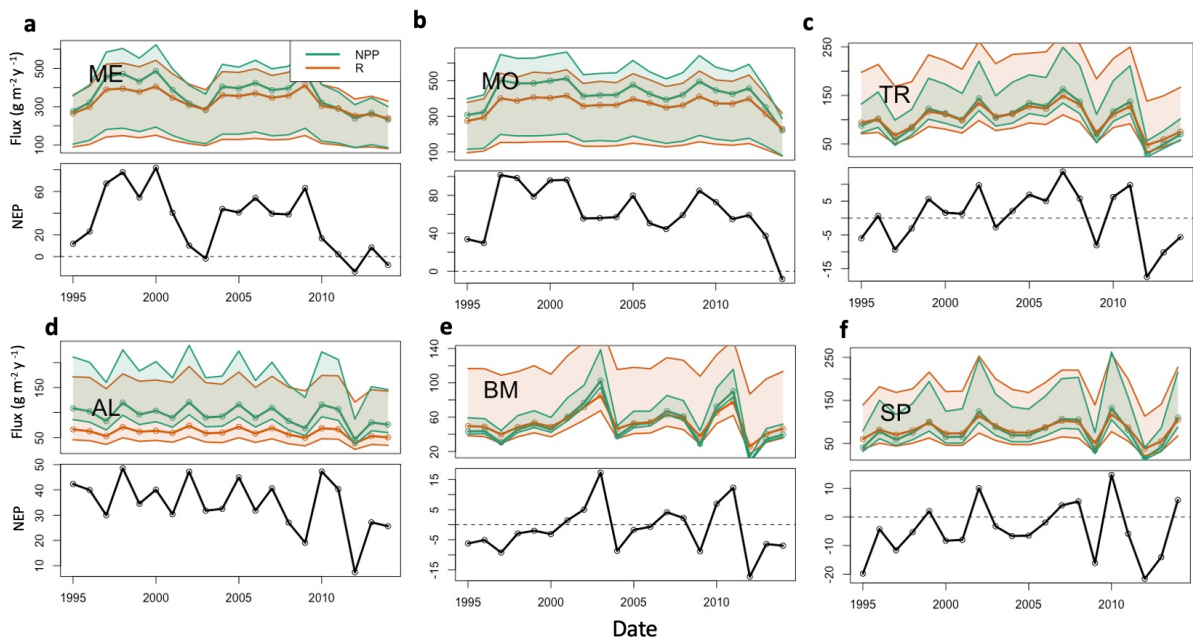
518 lowest in SP (5.25%).

519

27

Figure 5. Total annual budget, sources (left stacked bars) and fates (right stacked bars), of organic carbon (OC) in each lake over the study period. The OC sources include allochthonous OC (OC$_{ALLOCH}$) and autochthonous OC (OC$_{AUTOCH}$). The OC fates include burial of OC (OC$_{BURIAL}$), export of OC (OC$_{EXPORT}$), sediment respiration of OC (R$_{SED}$), and water column respiration of OC (R$_{WC}$). Standard error bars for the annual means are indicated for each source and fate as well. Note that the magnitudes of the y-axis differ among the lakes. A significance test comparing these fluxes across the study lakes can be found in SI Table 6.

The lakes show inter-annual variation in trophic state, as quantified by NEP (Fig. 6). Total respiration (water column and sediment) exceeds autochthony in SP, BM, and TR, indicating predominantly net heterotrophy for these systems. The remaining lakes (ME, MO, AL) are generally net autotrophic. The southern lakes (ME, MO) are net autotrophic (positive NEP) for the majority of the study years but became less autotrophic over the last five years of the study period (2010-2014). BM and SP are mostly net heterotrophic (negative NEP) over the study period with a few brief instances of net autotrophy. The strongest autotrophic signal for

28
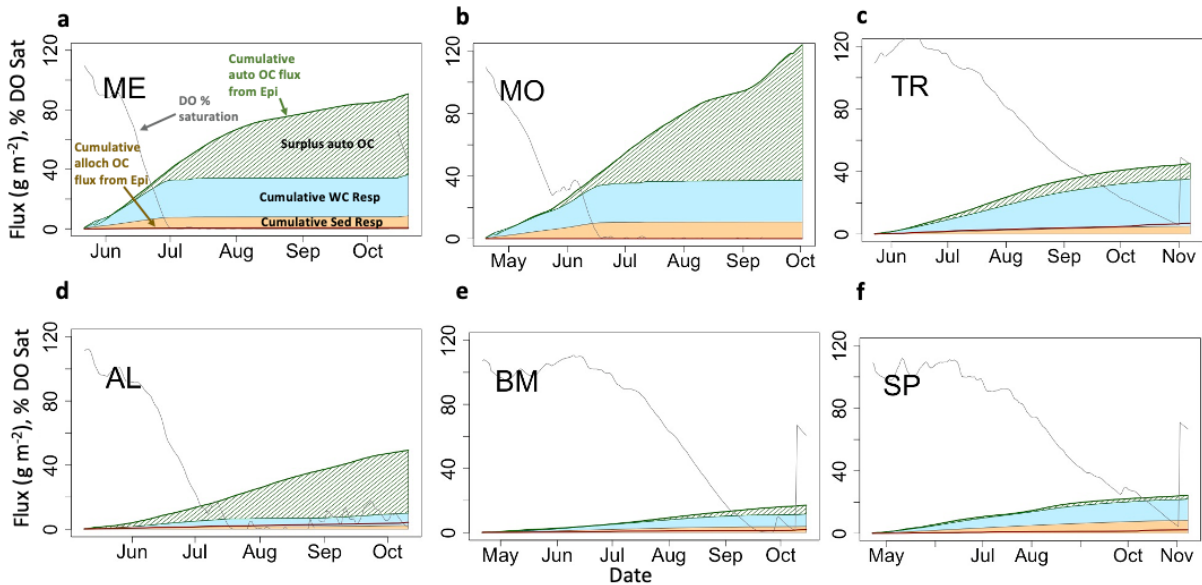
these lakes occurred around 2010. TR experienced prolonged periods of both autotrophy and

heterotrophy. AL is net autotrophic over the study period but had lower average NEP than

the southern lakes. ME, MO, and AL all have negative trends in NPP, but only ME and AL

were significant (p_value < 0.1, Mann-Kendall test) (SI Table 2). Of these three lakes, ME

and AL also have decreasing significant trends in annual total phosphorus concentration (SI

Table 2). No significant trends were found for NPP or total phosphorus in the other lakes

(MO, TR, BM, SP).

Figure 6. Time series of calibrated lake Net Primary Production (green), Total Respiration
(red) (top panels), and Net Ecosystem Production (NEP, bottom panels) for the six lakes: (a)
Lake Mendota; (b) Lake Monona; (c) Trout Lake; (d) Allequash Lake; (e) Big Muskellunge
Lake, and; (f) Sparkling Lake. Fluxes are in units of $gC\ m^{-2}y^{-1}$. Solid line represents
prediction based on best parameter estimates. Shaded regions represent prediction
uncertainty based on parameter ranges in Table 3. Shaded region for NEP not shown to
reduce axis limits and emphasize NEP pattern.

Hypolimnetic DO consumption during stratified periods was modeled as a function of the

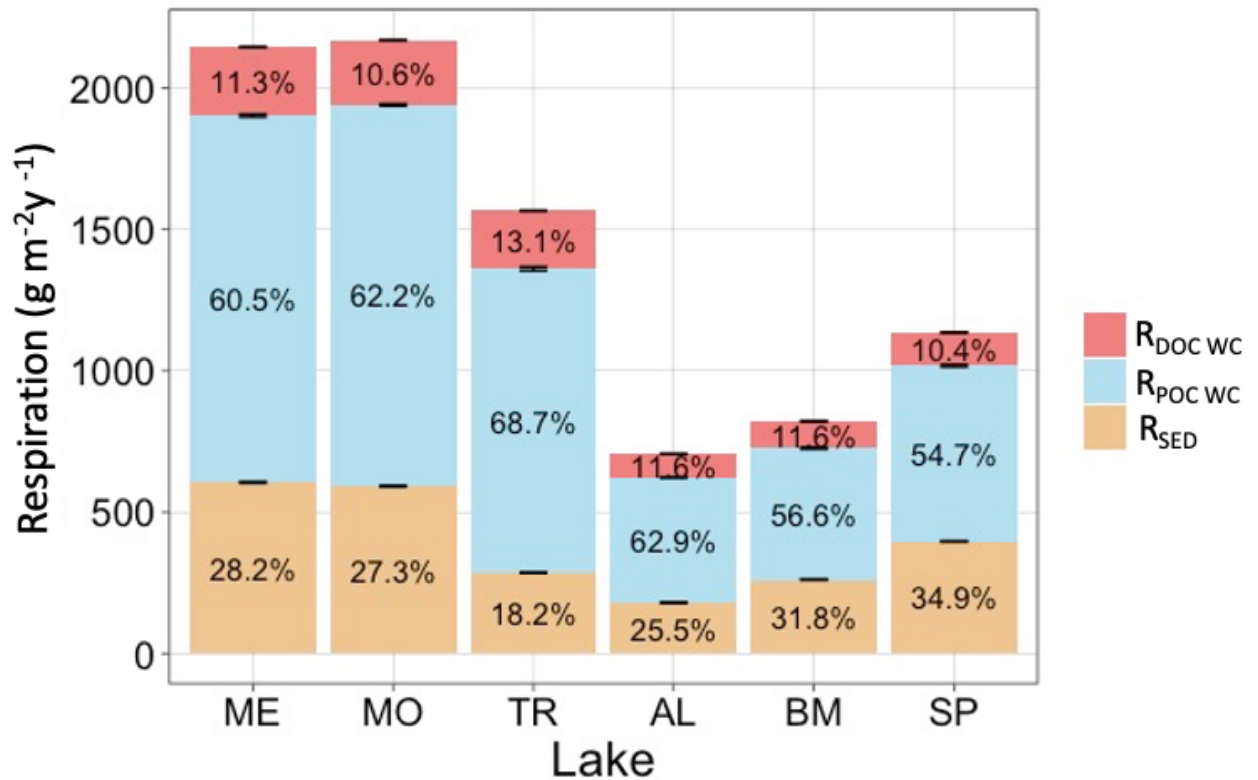two components of hypolimnetic respiration, hypolimnetic water column respiration and

29

556   hypolimnetic sediment respiration. Water column respiration contributes more than sediment

557   respiration to total hypolimnetic respiration in the southern lakes compared to the northern

558   lakes, with the exception of TR, where cumulative water column respiration is much larger

559   than cumulative sediment respiration. In ME and MO, the mass of summer autochthonous

560   POC entering the hypolimnion is similar to the total hypolimnetic OC mass respired for the

561   beginning of the stratified period (Fig. 7a-b; green line). Later in the stratified period, an

562   increase in epilimnetic POC and associated settling exceeds total hypolimnetic respiration

563   (Fig. 7a-b; green hashed area). This is due, in part, to lower respiration rates that occur once

564   DO (gray line) has been fully depleted, which occurs in early July for ME and late June for

565   MO. In BM and SP the total hypolimnetic respiration slightly exceeds autochthonous POC

566   inputs during parts of the stratified period, indicating the importance of allochthony in these

567   systems (Fig. 7c,f). BM shows that autochthonous POC entering the hypolimnion and total

568   hypolimnetic respiration are similar for much of the stratified period (Fig. 7d). AL is the only

569   lake to have autochthonous POC inputs consistently larger than total hypolimnetic respiration

570   during the stratified season. All lakes show that summer allochthonous POC entering the

571   hypolimnion is a small contribution to the overall hypolimnetic POC load.

572

30

Figure 7. Hypolimnetic dissolved oxygen, allochthonous (alloch) and autochthonous (auto) organic carbon loading, and respiration dynamics during one stratified period (2005) for each lake. Fluxes are cumulative $gC\ m^{-2}$ and DO is presented as percent saturation. Labels are in panel (a). Note that the cumulative water column (WC) and sediment (Sed) respiration fluxes are stacked, while other cumulative fluxes are not.

Respiration of autochthonous POC and sediment respiration account for most of the total hypolimnetic respiration in all lakes (Fig. 8). Respiration of DOC accounts for a relatively small proportion of total respiration. Total hypolimnetic respiration is higher in the southern lakes than the northern lakes. TR has the highest amount of hypolimnetic respiration for the northern lakes, and AL and BM have the least amounts of hypolimnetic respiration. Water column respiration contributed the most towards total hypolimnetic respiration in all lakes. Sediment respiration contributed the largest proportion towards total hypolimnetic respiration in BM and SP. DOC water column respiration was the smallest proportion of total hypolimnetic respiration in all six study lakes.

31

Figure 8. Total average annual hypolimnetic respiration, separated by percentages attributed to water column DOC ($R_{DOC\ WC}$), water column POC ($R_{POC\ WC}$), and sediment (R_{SED}) organic carbon sources. Standard error bars for the annual respiration values are indicated as well.

4 Discussion

4.1 Autochthonous and Allochthonous Loads

Autochthony was the dominant source of OC subsidizing hypolimnetic respiration in the

study lakes. The importance of autochthonous OC pools in ecosystem respiration was

surprising, given ample research highlighting the dominance of allochthonous OC in north

temperate lakes (Wilkinson et al. 2013; Hanson et al. 2011; Hanson et al. 2014). This

outcome emphasizes the utility of process-based models in studying mechanisms that discern

the relative contributions of different pools of organic matter to lake metabolism.

32

603   Autochthonous OC pools have higher turnover rates than allochthonous OC pools (Dordoni

604   et al., 2022) and often are lower in concentration than the more recalcitrant allochthonous

605   pools (Wilkinson et al. 2013). Thus, studies based on correlative relationships between lake

606   concentrations of organic matter and water quality metrics, likely overlook the importance of

607   more labile organic matter in driving observable ecosystem phenomena, such as gas flux and

608   formation of hypolimnetic anoxia (Evans et al., 2005; Feng et al., 2022). By quantifying

609   metabolism fluxes relevant to both OC pools, we can recreate shorter-term OC processes that

610   quantify high turnover of labile organic matter, which would typically be missed by

611   empirical studies based on monthly or annual observations.

612

613   Allochthony and autochthony are important to lake carbon cycling, but in ways that play out

614   at different time scales. Allochthonous OC has been well-established as an important factor

615   in driving negative NEP through a number of mechanisms (Wilkinson et al., 2013; Hanson et

616   al., 2014; Hanson et al., 2011). Allochthony contributes to water quality variables, such as

617   Secchi depth (Solomon et al. 2015), by providing the bulk of DOC in most lakes (Wilkinson

618   et al., 2013) and can drive persistent hypolimnetic anoxia in dystrophic lakes (Knoll et al.,

619   2018). In contrast, autochthony contributes to seasonal dynamics of water quality through

620   rapid changes in OC that can appear and disappear within a season. Within that seasonal time

621   frame, autochthonous POC settling from the epilimnion can drive hypolimnetic respiration,

622   thus controlling another key water quality metric, oxygen depletion. It is worth noting that

623   our model does not discern allochthonous and autochthonous sediment OC, however we

624   show that autochthonous OC makes up the largest proportion of OC loads in our study lakes

625   and therefore autochthony likely contributes substantially to the sediment OC pool. For

626   highly eutrophic lakes, the model results show excess autochthony stored in the sediments

627   which may carry into subsequent years, potentially providing additional substrate for

628   sediment respiration. Thus, understanding and predicting controls over hypolimnetic oxygen

629   depletion benefits from quantifying both allochthonous and autochthonous OC cycles.

630

631   Differences in trophic status, hydrologic residence time, and inflow sources help explain the

632   relative proportion of allochthonous versus autochthonous OC among lakes in our study.

633   Water residence times (Hotchkiss et al. 2018; McCullough et al. 2018) and surrounding land

634   cover (Hanson et al. 2014) have been shown to have a substantial impact on OC dynamics by

635   controlling allochthonous OC loading and NEP trends on lakes included in our study

636   (Hanson et al. 2014, McCullough et al. 2018). We built upon these ideas by recreating daily

637   watershed loading dynamics of POC and DOC from derived discharge data and incorporating

638   nutrient control over lake primary production by using high quality and long-term

639   observational data. The northern lakes are embedded in a forest and wetland landscape,

640   which are characteristic of having higher DOC than the urban and agricultural landscape of

641   the southern lakes (Creed et al., 2003). This creates variation in allochthonous loading across

642   the study lakes. Lake trophic state and productivity are a major control for autochthonous

643   production, which influences autochthonous loads across the study lakes as well. For lake

644   metrics that are comparable between studies, such as allochthonous loading and export,

645   allochthonous water column respiration, and total OC burial, our results were within 20% of

646   values in related studies (Hanson et al. 2014, McCullough et al. 2018).

34

647

4.2 Hypolimnetic Respiration

649 Given the importance of autochthonous POC to hypolimnetic respiration, we assume it

650 contributes substantially to both sediment respiration and respiration in the water column.

651 While previous work found that sediment respiration was the dominant respiration source for

652 lakes with depth ranges encompassed within our study (Steinsberger 2020), we found that

653 water column respiration was at least as important, if not more so. Differences in these

654 findings could be linked to uncertainty in the settling velocity of POC, due to lack of

655 empirical POC settling velocity measurements. Perhaps, POC mineralized in the hypolimnia

656 of our modeled lakes passes more quickly to the sediments in real ecosystems, shifting the

657 balance of respiration more toward the sediments. OC respiration can contribute substantially

658 to hypolimnetic DO depletion in both lakes and reservoirs (Beutel, 2003), and POC settling

659 velocities can be highly variable, suggesting that assumptions around vertical distribution of

660 lake POC deserve further investigation. Another possible explanation for these differences

661 could be that our model missed allochthonous POC loads from extreme events (Carpenter et

662 al., 2012), which can increase the amount of legacy OC stored in the sediments and increase

663 sediment respiration. Our model also does not account for reduced respiration rates due to

664 OC aging, which may explain our higher values of water column respiration. Finally, our

665 model includes entrainment as a possible oxygen source to the hypolimnion, which must be

666 offset by respiration to fit observed hypolimnetic DO changes. Any study that underestimates

667 DO sources to the hypolimnion likely underestimates total respiration.

668

35

669   Anaerobic mineralization of organic carbon is an important biogeochemical process and can

670   be a substantial carbon sink through methanogenesis (Maerki et al. 2009). Although

671   methanogenesis is not incorporated into our model, methane dissolved in the water column of

672   Lake Mendota is mostly oxidized (Hart 2017), thus contributing to the overall oxygen

673   demand, which is accounted for in our model. What remains unaccounted is ebullition of

674   methane, which is a carbon flux that is difficult to quantify (McClure et al. 2020). Future

675   metabolism studies that include these processes might find a decrease in annual OC burial

676   rates relative to rates in our study. Although we believe that ebullition is not a substantial

677   portion of the lake's carbon mass budget, that remains to be studied more carefully. As the

678   model accounts for DO consumption through calibration, the overall flux would not change

679   even if we link DO consumption to methane oxidation, only the process description would be

680   more realistic.

681

682   Our findings highlight the importance of autochthonous POC in hypolimnetic oxygen

683   depletion and suggest that related processes, such as the timing of nutrient loading, changes

684   in thermocline depth, or zooplankton grazing, could impact overall lake respiration dynamics

685   and anoxia formation (Schindler et al., 2016; Ladwig et al., 2021; Müller et al., 2012).

686

687   **4.3 Long-term Dynamics**

688   Although autochthonous OC dominated the loads across the study lakes, analysis of the long-

689   term OC dynamics supports the importance of allochthony in lakes. Net Ecosystem

690   Production (NEP) has been used to quantify heterotrophy and autotrophy in lakes (Odum

691 1956, Hanson et al. 2003, Cole et al. 2000, Lovett et al. 2006), and using this metric over

692 multiple decades allowed us to analyze long-term impacts of allochthony. TR, BM, and SP

693 fluctuated between heterotrophy and autotrophy, usually in tandem with trends in hydrology,

694 which acts as a main control of allochthonous OC. This suggests that allochthonous OC

695 inputs may be less important for seasonal anoxia but can still drive a lake toward negative

696 NEP and contribute to sediment carbon storage over long time periods. ME, MO, and AL

697 tended to become less autotrophic over time (Fig. 6), a pattern that coincided with significant

698 decreasing trends in mean epilimnetic total phosphorus concentrations for ME and AL (SI

699 Fig. 5). In our model, NPP and phosphorus are directly related, so decreases in phosphorus

700 are likely to cause decreases in NEP. Short-term respiration of autochthonous POC can

701 account for rapid decreases in hypolimnetic DO, but allochthonous POC, which tends to be

702 more recalcitrant, provides long-term subsidy of ecosystem respiration that can result in

703 long-term net heterotrophy. Thus, it's critical to understand and quantify both the rapid

704 internal cycling based on autochthony and the long and slow turnover of allochthony.

705

706 Through explicitly simulating the cycling of both allochthony and autochthony, we can

707 expand our conceptual model of metabolism to better understand time dynamics of lake

708 water quality at the ecosystem scale. Autochthony has pronounced seasonal dynamics,

709 typically associated with the temporal variability of phytoplankton communities and the

710 growth and senescence of macrophytes (Rautio et al., 2011). While allochthony can also have

711 strong seasonal patterns associated with leaf litter input, pollen blooms, and spring runoff

712 events, its more recalcitrant nature leads to a less pronounced seasonal signal at the

37

713 ecosystem scale (Wilkinson et al., 2013, Tranvik 1998). When considered together, it seems

714 that allochthony underlies long and slow changes in metabolism patterns, while autochthony

715 overlays strong seasonality. Both OC pools are important for ecosystem scale metabolism

716 processes, and their consequences are evident at different time scales. Therefore, the

717 interactions of both OC sources and their influences on water quality patterns deserve further

718 investigation.

719

720 Autochthonous OC control over hypolimnetic respiration should be a primary consideration

721 for understanding the influence of OC on ecosystem dynamics. Hypolimnetic oxygen

722 depletion and anoxia in productive lakes can be mitigated by reducing autochthonous

723 production of OC, which we show is mainly driven by nutrient availability. This study also

724 identifies the need for a better understanding of internal and external OC loads in lakes.

725 Previous studies have found heterotrophic behavior in less productive lakes, but our findings

726 highlight the importance of autochthony in these lakes, especially for shorter-time scale

727 processes that can be missed by looking at broad annual patterns. By using a one-

728 dimensional, two-layer model, we are able to also understand how surface metabolism

729 processes can impact bottom layer dynamics, which would not be possible with a zero-

730 dimensional model. Looking forward, we believe that our understanding of these processes

731 could be improved by building a coupled watershed - metabolism model to more closely

732 explore causal relations between watershed hydrology, nutrient dynamics, and lake

733 morphometry.

734

735

736

747 *Author Contributions*
748 AD, PH, RL, and CB assisted with model development and analysis of results. AD and PH
749 prepared the manuscript with contributions from RL, CB, and EA.
750
751 *Competing Interests*
752 The authors declare that they have no conflict of interest.
753

References

764 <u>References</u>

765 Amon, R. M. W., & Benner, R. (1996). Photochemical and microbial consumption of

766   dissolved organic carbon and dissolved oxygen in the Amazon River system.

767   *Geochimica et Cosmochimica Acta*, *60*(10), 1783–1792. <u>https://doi.org/10.1016/0016-</u>

768   <u>7037(96)00055-5</u>

769 Beutel, M. W. (2003). Hypolimnetic Anoxia and Sediment Oxygen Demand in California

770   Drinking Water Reservoirs. *Lake and Reservoir Management*, *19*(3), 208–221.

771   <u>https://doi.org/10.1080/07438140309354086</u>

772 Bryant, L. D., Hsu-Kim, H., Gantzer, P. A., & Little, J. C. (2011). Solving the problem at the

773   source: Controlling Mn release at the sediment-water interface via hypolimnetic

774   oxygenation. *Water Research*, *45*(19), 6381–6392.

775   <u>https://doi.org/10.1016/j.watres.2011.09.030</u>

776 Cardille, J. A., Carpenter, S. R., Coe, M. T., Foley, J. A., Hanson, P. C., Turner, M. G., &

777   Vano, J. A. (2007). Carbon and water cycling in lake-rich landscapes: Landscape

778   connections, lake hydrology, and biogeochemistry. *Journal of Geophysical Research*,

779   *112*(G2), G02031. <u>https://doi.org/10.1029/2006JG000200</u>

780 Carpenter, S., Arrow, K., Barrett, S., Biggs, R., Brock, W., Crépin, A.-S., Engström, G.,

781   Folke, C., Hughes, T., Kautsky, N., Li, C.-Z., McCarney, G., Meng, K., Mäler, K.-G.,

782   Polasky, S., Scheffer, M., Shogren, J., Sterner, T., Vincent, J., … Zeeuw, A. (2012).

783   General Resilience to Cope with Extreme Events. *Sustainability*, *4*(12), 3248–3259.

784   <u>https://doi.org/10.3390/su4123248</u>

785 Carpenter, S. R., Benson, B. J., Biggs, R., Chipman, J. W., Foley, J. A., Golding, S. A.,

786   Hammer, R. B., Hanson, P. C., Johnson, P. T. J., Kamarainen, A. M., Kratz, T. K.,

787   Lathrop, R. C., McMahon, K. D., Provencher, B., Rusak, J. A., Solomon, C. T., Stanley,

788   E. H., Turner, M. G., Vander Zanden, M. J., … Yuan, H. (2007). Understanding

789   Regional Change: A Comparison of Two Lake Districts. *BioScience*, *57*(4), 323–335.

790   https://doi.org/10.1641/B570407

791 Catalán, N., Marcé, R., Kothawala, D. N., & Tranvik, Lars. J. (2016). Organic carbon

792   decomposition rates controlled by water retention time across inland waters. *Nature

793   Geoscience*, *9*(7), 501–504. https://doi.org/10.1038/ngeo2720

794 Cole, G., & Weihe, P. (2016). *Textbook of Limnology*. Waveland Press, Inc.

795 Cole, J. J., & Caraco, N. F. (1998). Atmospheric exchange of carbon dioxide in a low-wind

796   oligotrophic lake measured by the addition of SF_6. *Limnology and Oceanography*,

797   *43*(4), 647–656. https://doi.org/10.4319/lo.1998.43.4.0647

798 Cole, J. J., Carpenter, S. R., Kitchell, J. F., & Pace, M. L. (2002). Pathways of organic carbon

799   utilization in small lakes: Results from a whole-lake ^{13}C addition and coupled model.

800   *Limnology and Oceanography*, *47*(6), 1664–1675.

801   https://doi.org/10.4319/lo.2002.47.6.1664

802 Cole, J. J., Pace, M. L., Carpenter, S. R., & Kitchell, J. F. (2000). Persistence of net

803   heterotrophy in lakes during nutrient addition and food web manipulations. *Limnology

804   and Oceanography*, *45*(8), 1718–1730. https://doi.org/10.4319/lo.2000.45.8.1718

805

806 Creed, I. F., Sanford, S. E., Beall, F. D., Molot, L. A., & Dillon, P. J. (2003). Cryptic

807 wetlands: Integrating hidden wetlands in regression models of the export of dissolved

808 organic carbon from forested landscapes. *Hydrological Processes*, *17*(18), 3629–3648.

809 https://doi.org/10.1002/hyp.1357

810 Delany, A. (2022). *Modeled Organic Carbon, Dissolved Oxygen, and Secchi for six*

811 *Wisconsin Lakes, 1995-2014* [Data set]. Environmental Data Initiative.

812 https://doi.org/10.6073/PASTA/1B5B947999AA2F9E0E95C91782B36EE9

813 Dordoni, M., Seewald, M., Rinke, K., van Geldern, R., Schmidmeier, J., & Barth, J. A. C.

814 (2022). *Mineralization of autochthonous particulate organic carbon is a fast channel of*

815 *organic matter turnover in Germany's largest drinking water reservoir* [Preprint].

816 Biogeochemistry: Stable Isotopes & Other Tracers. https://doi.org/10.5194/bg-

817 2022-154

818 Evans, C. D., Monteith, D. T., & Cooper, D. M. (2005). Long-term increases in surface water

819 dissolved organic carbon: Observations, possible causes and environmental impacts.

820 *Environmental Pollution*, *137*(1), 55–71. https://doi.org/10.1016/j.envpol.2004.12.031

821 Feng, L., Zhang, J., Fan, J., Wei, L., He, S., & Wu, H. (2022). Tracing dissolved organic

822 matter in inflowing rivers of Nansi Lake as a storage reservoir: Implications for water-

823 quality control. *Chemosphere*, *286*, 131624.

824 https://doi.org/10.1016/j.chemosphere.2021.131624

825

826

827   Goudsmit, G.-H., Burchard, H., Peeters, F., & Wüest, A. (2002). Application of k-ϵ

828   turbulence models to enclosed basins: The role of internal seiches: APPLICATION OF

829   k-ϵ TURBULENCE MODELS. *Journal of Geophysical Research: Oceans*, *107*(C12),

830   23-1-23–13. https://doi.org/10.1029/2001JC000954

831   Hanson, P. C., Bade, D. L., Carpenter, S. R., & Kratz, T. K. (2003). Lake metabolism:

832   Relationships with dissolved organic carbon and phosphorus. *Limnology and*

833   *Oceanography*, *48*(3), 1112–1119. https://doi.org/10.4319/lo.2003.48.3.1112

834   Hanson, P.C., Carpenter S.R., Cardille, J.A, Coe, M.T., & Winslow, L.A. (2007). Small lakes

835   dominate a random sample of reginal lake characteristics. *Freshwater Biology* 52(5),

836   814–822. https://doi.org/10.1111/j.1365-2427.2007.01730.x

837   Hanson, P. C., Buffam, I., Rusak, J. A., Stanley, E. H., & Watras, C. (2014). Quantifying lake

838   allochthonous organic carbon budgets using a simple equilibrium model. *Limnology and*

839   *Oceanography*, *59*(1), 167–181. https://doi.org/10.4319/lo.2014.59.1.0167

840   Hanson, P. C., Hamilton, D. P., Stanley, E. H., Preston, N., Langman, O. C., & Kara, E. L.

841   (2011). Fate of Allochthonous Dissolved Organic Carbon in Lakes: A Quantitative

842   Approach. *PLoS ONE*, *6*(7), e21884. https://doi.org/10.1371/journal.pone.0021884

843   Hanson, P. C., Pace, M. L., Carpenter, S. R., Cole, J. J., & Stanley, E. H. (2015). Integrating

844   Landscape Carbon Cycling: Research Needs for Resolving Organic Carbon Budgets of

845   Lakes. *Ecosystems*, *18*(3), 363–375. https://doi.org/10.1007/s10021-014-9826-9

846   Hanson, P. C., Pollard, A. I., Bade, D. L., Predick, K., Carpenter, S. R., & Foley, J. A.

847   (2004). A model of carbon evasion and sedimentation in temperate lakes:

848   LANDSCAPE-LAKE CARBON CYCLING MODEL. *Global Change Biology*, *10*(8),

849   1285–1298. https://doi.org/10.1111/j.1529-8817.2003.00805.x

850

851 Hanson, P. C., Stillman, A. B., Jia, X., Karpatne, A., Dugan, H. A., Carey, C. C., Stachelek,

852   J., Ward, N. K., Zhang, Y., Read, J. S., & Kumar, V. (2020). Predicting lake surface

853   water phosphorus dynamics using process-guided machine learning. *Ecological*

854   *Modelling*, *430*, 109136. https://doi.org/10.1016/j.ecolmodel.2020.109136

855 Hart, J., Dugan, H., Carey, C., Stanley, E., & Hanson, P. (2019). *Lake Mendota Carbon and*

856   *Greenhouse Gas Measurements at North Temperate Lakes LTER 2016* [Data set].

857   Environmental Data Initiative.

858   https://doi.org/10.6073/PASTA/170E5BA0ED09FE3D5837EF04C47E432E

859 Hipsey, M. R. (2022). *Modelling Aquatic Eco-Dynamics: Overview of the AED modular*

860   *simulation platform*. https://doi.org/10.5281/ZENODO.6516222

861 Hipsey, M. R., Bruce, L. C., Boon, C., Busch, B., Carey, C. C., Hamilton, D. P., Hanson, P.

862   C., Read, J. S., de Sousa, E., Weber, M., & Winslow, L. A. (2019). A General Lake

863   Model (GLM 3.0) for linking with high-frequency sensor data from the Global Lake

864   Ecological Observatory Network (GLEON). *Geoscientific Model Development*, *12*(1),

865   473–523. https://doi.org/10.5194/gmd-12-473-2019

866 Hoffman, A. R., Armstrong, D. E., & Lathrop, R. C. (2013). Influence of phosphorus

867   scavenging by iron in contrasting dimictic lakes. *Canadian Journal of Fisheries and*

868   *Aquatic Sciences*, *70*(7), 941–952. https://doi.org/10.1139/cjfas-2012-0391

869   Hotchkiss, E. R., Sadro, S., & Hanson, P. C. (2018). Toward a more integrative perspective

870   on carbon metabolism across lentic and lotic inland waters. *Limnology and*

871   *Oceanography Letters*, *3*(3), 57–63. https://doi.org/10.1002/lol2.10081

872   Houser, J. N., Bade, D. L., Cole, J. J., & Pace, M. L. (2003). The dual influences of dissolved

873   organic carbon on hypolimnetic metabolism: Organic substrate and photosynthetic

874   reduction. *Biogeochemistry*, *64*(2), 247–269. https://doi.org/10.1023/A:1024933931691

875   Hunt, R. J., & Walker, J. F. (2017). *2016 Update to the GSFLOW groundwater-surface water*

876   *model for the Trout Lake Watershed*. https://doi.org/10.5066/F7M32SZ2

877   Hunt, R. J., Walker, J. F., Selbig, W. R., Westenbroek, S. M., & Regan, R. S. (2013).

878   *Simulation of Climate-Change Effects on Streamflow, Lake Water Budgets, and Stream*

879   *Temperature Using GSFLOW and SNTEMP, Trout Lake Watershed, Wisconsin*. United

880   States Geological Survey.

881   Jane, S. F., Hansen, G. J. A., Kraemer, B. M., Leavitt, P. R., Mincer, J. L., North, R. L., Pilla,

882   R. M., Stetler, J. T., Williamson, C. E., Woolway, R. I., Arvola, L., Chandra, S.,

883   DeGasperi, C. L., Diemer, L., Dunalska, J., Erina, O., Flaim, G., Grossart, H.-P.,

884   Hambright, K. D., … Rose, K. C. (2021). Widespread deoxygenation of temperate lakes.

885   *Nature*, *594*(7861), 66–70. https://doi.org/10.1038/s41586-021-03550-y

886   Jansson, M., Bergström, A.-K., Blomqvist, P., & Drakare, S. (2000). ALLOCHTHONOUS

887   ORGANIC CARBON AND PHYTOPLANKTON/BACTERIOPLANKTON

888   PRODUCTION RELATIONSHIPS IN LAKES. *Ecology*, *81*(11), 3250–3255.

889   https://doi.org/10.1890/0012-9658(2000)081[3250:AOCAPB]2.0.CO;2

890   Jenny, J.-P., Francus, P., Normandeau, A., Lapointe, F., Perga, M.-E., Ojala, A.,

891   Schimmelmann, A., & Zolitschka, B. (2016). Global spread of hypoxia in freshwater

892   ecosystems during the last three centuries is caused by rising local human pressure.

893   *Global Change Biology*, *22*(4), 1481–1489. https://doi.org/10.1111/gcb.13193

894   Jenny, J.-P., Normandeau, A., Francus, P., Taranu, Z. E., Gregory-Eaves, I., Lapointe, F.,

895   Jautzy, J., Ojala, A. E. K., Dorioz, J.-M., Schimmelmann, A., & Zolitschka, B. (2016).

896   Urban point sources of nutrients were the leading cause for the historical spread of

897   hypoxia across European lakes. *Proceedings of the National Academy of Sciences*,

898   *113*(45), 12655–12660. https://doi.org/10.1073/pnas.1605480113

899   Knoll, L. B., Williamson, C. E., Pilla, R. M., Leach, T. H., Brentrup, J. A., & Fisher, T. J.

900   (2018). Browning-related oxygen depletion in an oligotrophic lake. *Inland Waters*, *8*(3),

901   255–263. https://doi.org/10.1080/20442041.2018.1452355

902   Kraemer, B. M., Chandra, S., Dell, A. I., Dix, M., Kuusisto, E., Livingstone, D. M.,

903   Schladow, S. G., Silow, E., Sitoki, L. M., Tamatamah, R., & McIntyre, P. B. (2017).

904   Global patterns in lake ecosystem responses to warming based on the temperature

905   dependence of metabolism. *Global Change Biology*, *23*(5), 1881–1890.

906   https://doi.org/10.1111/gcb.13459

907   Ladwig, R., Hanson, P. C., Dugan, H. A., Carey, C. C., Zhang, Y., Shu, L., Duffy, C. J., &

908   Cobourn, K. M. (2021). Lake thermal structure drives interannual variability in summer

909   anoxia dynamics in a eutrophic lake over 37 years. *Hydrology and Earth System

910   Sciences*, *25*(2), 1009–1032. https://doi.org/10.5194/hess-25-1009-2021

47

911   Lathrop, R., & Carpenter, S. (2014). Water quality implications from three decades of

912   phosphorus loads and trophic dynamics in the Yahara chain of lakes. *Inland Waters*,

913   *4*(1), 1–14. https://doi.org/10.5268/IW-4.1.680

914   Lei, R., Leppäranta, M., Erm, A., Jaatinen, E., & Pärn, O. (2011). Field investigations of

915   apparent optical properties of ice cover in Finnish and Estonian lakes in winter 2009.

916   *Estonian Journal of Earth Sciences*, *60*(1), 50. https://doi.org/10.3176/earth.2011.1.05

917   Livingstone, D. M., & Imboden, D. M. (1996). The prediction of hypolimnetic oxygen

918   profiles: A plea for a deductive approach. *Canadian Journal of Fisheries and Aquatic*

919   *Sciences*, *53*(4), 924–932. https://doi.org/10.1139/f95-230

920   Loose, B., & Schlosser, P. (2011). Sea ice and its effect on CO_2 flux between the atmosphere

921   and the Southern Ocean interior. *Journal of Geophysical Research: Oceans*, *116*(C11),

922   2010JC006509. https://doi.org/10.1029/2010JC006509

923   Lovett, G. M., Cole, J. J., & Pace, M. L. (2006). Is Net Ecosystem Production Equal to

924   Ecosystem Carbon Accumulation? *Ecosystems*, *9*(1), 152–155.

925   https://doi.org/10.1007/s10021-005-0036-3

926   Maerki, M., Müller, B., Dinkel, C., & Wehrli, B. (2009). Mineralization pathways in lake

927   sediments with different oxygen and organic carbon supply. *Limnology and*

928   *Oceanography*, *54*(2), 428–438. https://doi.org/10.4319/lo.2009.54.2.0428

929   Magee, M. R., McIntyre, P. B., Hanson, P. C., & Wu, C. H. (2019). Drivers and Management

930   Implications of Long-Term Cisco Oxythermal Habitat Decline in Lake Mendota, WI.

931   *Environmental Management*, *63*(3), 396–407. https://doi.org/10.1007/s00267-018-

932   01134-7

48

933

934

Magnuson, J., Carpenter, S., & Stanley, E. (2020). *North Temperate Lakes LTER: Chemical*

   Limnology of Primary Study Lakes: Nutrients, pH and Carbon 1981 - current [Data set].

   Environmental Data Initiative.

   https://doi.org/10.6073/PASTA/8359D27BBD91028F222D923A7936077D

Magnuson, J. J., Benson, B. J., & Kratz, T. K. (2006). *Long-term dynamics of lakes in the*

   landscape: Long-term ecological research on north temperate lakes. Oxford University

   Press on Demand.

Magnuson, J. J., Carpenter, S. R., & Stanley, E. H. (2022). *North Temperate Lakes LTER:*

   Physical Limnology of Primary Study Lakes 1981 - current [Data set]. Environmental

   Data Initiative.

   https://doi.org/10.6073/PASTA/925D94173F35471F699B5BC343AA1128

McClure, R. P., Lofton, M. E., Chen, S., Krueger, K. M., Little, J. C., & Carey, C. C. (2020).

   The Magnitude and Drivers of Methane Ebullition and Diffusion Vary on a Longitudinal

   Gradient in a Small Freshwater Reservoir. *Journal of Geophysical Research:*

   Biogeosciences, *125*(3). https://doi.org/10.1029/2019JG005205

McCullough, I. M., Dugan, H. A., Farrell, K. J., Morales-Williams, A. M., Ouyang, Z.,

   Roberts, D., Scordo, F., Bartlett, S. L., Burke, S. M., Doubek, J. P., Krivak-Tetley, F. E.,

   Skaff, N. K., Summers, J. C., Weathers, K. C., & Hanson, P. C. (2018). Dynamic

   modeling of organic carbon fates in lake ecosystems. *Ecological Modelling*, *386*, 71–82.

   https://doi.org/10.1016/j.ecolmodel.2018.08.009

955

956 Mi, C., Shatwell, T., Ma, J., Wentzky, V. C., Boehrer, B., Xu, Y., & Rinke, K. (2020). The

957   formation of a metalimnetic oxygen minimum exemplifies how ecosystem dynamics

958   shape biogeochemical processes: A modelling study. *Water Research*, *175*, 115701.

959   https://doi.org/10.1016/j.watres.2020.115701

960 Morris, M. D. (1991). Factorial Sampling Plans for Preliminary Computational Experiments.

961   *Technometrics*, *33*(2), 161–174. https://doi.org/10.1080/00401706.1991.10484804

962 Müller, B., Bryant, L. D., Matzinger, A., & Wüest, A. (2012). Hypolimnetic Oxygen

963   Depletion in Eutrophic Lakes. *Environmental Science & Technology*, *46*(18), 9964–

964   9971. https://doi.org/10.1021/es301422r

965 Nürnberg, G. K. (1995). Quantifying anoxia in lakes. *Limnology and Oceanography*, *40*(6),

966   1100–1111. https://doi.org/10.4319/lo.1995.40.6.1100

967 Nürnberg, G. K. (2004). Quantified Hypoxia and Anoxia in Lakes and Reservoirs. *The*

968   *Scientific World JOURNAL*, *4*, 42–54. https://doi.org/10.1100/tsw.2004.5

969 Odum, H. T. (1956). Primary Production in Flowing Waters. *Limnology and Oceanography*,

970   *1*(2), 102–117. https://doi.org/10.4319/lo.1956.1.2.0102

971 Platt, T., Gallegos, C., & Harrison, W. (1980). Photoinhibition of photosynthesis in natural

972   assemblages of marine phytoplankton. *Journal of Marine Research*, *38*(4), 687–701.

973 Prairie, Y. T., Bird, D. F., & Cole, J. J. (2002). The summer metabolic balance in the

974   epilimnion of southeastern Quebec lakes. *Limnology and Oceanography*, *47*(1), 316–

975   321. https://doi.org/10.4319/lo.2002.47.1.0316

976   Qu, Y., & Duffy, C. J. (2007). A semidiscrete finite volume formulation for multiprocess

977   watershed simulation: MULTIPROCESS WATERSHED SIMULATION. *Water*

978   *Resources Research*, *43*(8). https://doi.org/10.1029/2006WR005752

979   Rautio, M., Mariash, H., & Forsström, L. (2011). Seasonal shifts between autochthonous and

980   allochthonous carbon contributions to zooplankton diets in a subarctic lake. *Limnology*

981   *and Oceanography*, *56*(4), 1513–1524. https://doi.org/10.4319/lo.2011.56.4.1513

982   Read, J. S., Hamilton, D. P., Jones, I. D., Muraoka, K., Winslow, L. A., Kroiss, R., Wu, C.

983   H., & Gaiser, E. (2011). Derivation of lake mixing and stratification indices from high-

984   resolution lake buoy data. *Environmental Modelling & Software*, *26*(11), 1325–1336.

985   https://doi.org/10.1016/j.envsoft.2011.05.006

986   Read, J. S., Zwart, J. A., Kundel, H., Corson-Dosch, H. R., Hansen, G. J. A., Vitense, K.,

987   Appling, A. P., Oliver, S. K., & Platt, L. (2021). *Data release: Process-based*

988   *predictions of lake water temperature in the Midwest US* [Data set]. U.S. Geological

989   Survey. https://doi.org/10.5066/P9CA6XP8

990   Reynolds, C. S., Oliver, R. L., & Walsby, A. E. (1987). Cyanobacterial dominance: The role

991   of buoyancy regulation in dynamic lake environments. *New Zealand Journal of Marine*

992   *and Freshwater Research*, *21*(3), 379–390.

993   https://doi.org/10.1080/00288330.1987.9516234

994   Rhodes, J., Hetzenauer, H., Frassl, M. A., Rothhaupt, K.-O., & Rinke, K. (2017). Long-term

995   development of hypolimnetic oxygen depletion rates in the large Lake Constance.

996   *Ambio*, *46*(5), 554–565. https://doi.org/10.1007/s13280-017-0896-8

997   Richardson, D. C., Carey, C. C., Bruesewitz, D. A., & Weathers, K. C. (2017). Intra- and

998   inter-annual variability in metabolism in an oligotrophic lake. *Aquatic Sciences*, *79*(2),

999   319–333. https://doi.org/10.1007/s00027-016-0499-7

1000   Rippey, B., & McSorley, C. (2009). Oxygen depletion in lake hypolimnia. *Limnology and*

1001   *Oceanography*, *54*(3), 905–916. https://doi.org/10.4319/lo.2009.54.3.0905

1002   Schindler, D. W., Carpenter, S. R., Chapra, S. C., Hecky, R. E., & Orihel, D. M. (2016).

1003   Reducing Phosphorus to Curb Lake Eutrophication is a Success. *Environmental Science*

1004   *& Technology*, *50*(17), 8923–8929. https://doi.org/10.1021/acs.est.6b02204

1005   Snortheim, C. A., Hanson, P. C., McMahon, K. D., Read, J. S., Carey, C. C., & Dugan, H. A.

1006   (2017). Meteorological drivers of hypolimnetic anoxia in a eutrophic, north temperate

1007   lake. *Ecological Modelling*, *343*, 39–53.

1008   https://doi.org/10.1016/j.ecolmodel.2016.10.014

1009   Sobek, S., Tranvik, L. J., Prairie, Y. T., Kortelainen, P., & Cole, J. J. (2007). Patterns and

1010   regulation of dissolved organic carbon: An analysis of 7,500 widely distributed lakes.

1011   *Limnology and Oceanography*, *52*(3), 1208–1219.

1012   https://doi.org/10.4319/lo.2007.52.3.1208

1013   Soetaert, K., & Petzoldt, T. (2010). Inverse Modelling, Sensitivity and Monte Carlo Analysis

1014   in *R* Using Package **FME**. *Journal of Statistical Software*, *33*(3).

1015   https://doi.org/10.18637/jss.v033.i03

1016

1017

1018   Solomon, C. T., Bruesewitz, D. A., Richardson, D. C., Rose, K. C., Van De Bogert, M. C.,

1019   Hanson, P. C., Kratz, T. K., Larget, B., Adrian, R., Babin, B. L., Chiu, C.-Y., Hamilton,

1020   D. P., Gaiser, E. E., Hendricks, S., Istvànovics, V., Laas, A., O'Donnell, D. M., Pace, M.

1021   L., Ryder, E., … Zhu, G. (2013). Ecosystem respiration: Drivers of daily variability and

1022   background respiration in lakes around the globe. *Limnology and Oceanography*, *58*(3),

1023   849–866. https://doi.org/10.4319/lo.2013.58.3.0849

1024   Solomon, C. T., Jones, S. E., Weidel, B. C., Buffam, I., Fork, M. L., Karlsson, J., Larsen, S.,

1025   Lennon, J. T., Read, J. S., Sadro, S., & Saros, J. E. (2015). Ecosystem Consequences of

1026   Changing Inputs of Terrestrial Dissolved Organic Matter to Lakes: Current Knowledge

1027   and Future Challenges. *Ecosystems*, *18*(3), 376–389. https://doi.org/10.1007/s10021-

1028   015-9848-y

1029   Staehr, P. A., Bade, D., Van de Bogert, M. C., Koch, G. R., Williamson, C., Hanson, P.,

1030   Cole, J. J., & Kratz, T. (2010). Lake metabolism and the diel oxygen technique: State of

1031   the science: Guideline for lake metabolism studies. *Limnology and Oceanography:*

1032   *Methods*, *8*(11), 628–644. https://doi.org/10.4319/lom.2010.8.0628

1033   Steinsberger, T., Schwefel, R., Wüest, A., & Müller, B. (2020). Hypolimnetic oxygen

1034   depletion rates in deep lakes: Effects of trophic state and organic matter accumulation.

1035   *Limnology and Oceanography*, *65*(12), 3128–3138. https://doi.org/10.1002/lno.11578

1036   Thorp, J. H., & Delong, M. D. (2002). Dominance of autochthonous autotrophic carbon in

1037   food webs of heterotrophic rivers. *Oikos*, *96*(3), 543–550.

1038   https://doi.org/10.1034/j.1600-0706.2002.960315.x

53

1039   Toming, K., Kotta, J., Uuemaa, E., Sobek, S., Kutser, T., & Tranvik, L. J. (2020). Predicting

1040   lake dissolved organic carbon at a global scale. *Scientific Reports*, *10*(1), 8471.

1041   https://doi.org/10.1038/s41598-020-65010-3

1042   Tranvik, L. J. (1998). Degradation of Dissolved Organic Matter in Humic Waters by

1043   Bacteria. In D. O. Hessen & L. J. Tranvik (Eds.), *Aquatic Humic Substances* (Vol. 133,

1044   pp. 259–283). Springer Berlin Heidelberg. https://doi.org/10.1007/978-3-662-03736-

1045   2_11

1046   Webster, K. E., Kratz, T. K., Bowser, C. J., Magnuson, J. J., & Rose, W. J. (1996). The

1047   influence of landscape position on lake chemical responses to drought in northern

1048   Wisconsin. *Limnology and Oceanography*, *41*(5), 977–984.

1049   https://doi.org/10.4319/lo.1996.41.5.0977

1050   Wilkinson, G. M., Pace, M. L., & Cole, J. J. (2013). Terrestrial dominance of organic matter

1051   in north temperate lakes: ORGANIC MATTER COMPOSITION IN LAKES. *Global

1052   Biogeochemical Cycles*, *27*(1), 43–51. https://doi.org/10.1029/2012GB004453

1053   Williamson, C. E., Dodds, W., Kratz, T. K., & Palmer, M. A. (2008). Lakes and streams as

1054   sentinels of environmental change in terrestrial and atmospheric processes. *Frontiers in

1055   Ecology and the Environment*, *6*(5), 247–254. https://doi.org/10.1890/070140

1056   Winslow, L. A., Zwart, J. A., Batt, R. D., Dugan, H. A., Woolway, R. I., Corman, J. R.,

1057   Hanson, P. C., & Read, J. S. (2016). LakeMetabolizer: An R package for estimating lake

1058   metabolism from free-water oxygen using diverse statistical models. *Inland Waters*,

1059   *6*(4), 622–636. https://doi.org/10.1080/IW-6.4.883

1060